

COMPARISON OF ACTIVE AND PASSIVE DANCERS FOR  
PERIODIC TENSION DISTURBANCE ATTENUATION IN WEB  
PROCESSING LINES

By

SESHADRI KUPPUSWAMY

Bachelor of Engineering

Rajiv Gandhi Institute of Technology

University of Mumbai

Mumbai, India

1997

Submitted to the Faculty of the  
Graduate College of the  
Oklahoma State University  
in partial fulfillment of  
the requirements for  
the Degree of  
MASTER OF SCIENCE  
December, 2004

COMPARISON OF ACTIVE AND PASSIVE DANCERS FOR  
PERIODIC TENSION DISTURBANCE ATTENUATION IN WEB  
PROCESSING LINES

Thesis Approved:

Dr. Prabhakar R. Pagilla

---

Thesis Adviser

Dr. Eduardo A. Misawa

---

Committee Member

Dr. Gary E. Young

---

Committee Member

Dr. A. Gordon Emslie

---

Dean of the Graduate College

## ACKNOWLEDGMENTS

For the successful completion of this thesis, primarily I would like to thank Dr. Prabhakar R. Pagilla, for his guidance and help. His expertise in the subject matter and his vision to develop a new approach for the problem discussed, was my primary motivation. I would also like to thank my committee members, Dr. Eduardo A. Misawa for the knowledge on Non-linear Systems, I gained in his classes and Dr. Gary E. Young for enhancing my programming and Data Acquisition Skills.

I would also like to thank my colleagues, Ramamurthy Dwivedula, Ashok Dubey, Nilesh Siraskar, Ryan Ratliff, Anil Abbaraju and Aravind Seshadri for their timely help during various stages of my research.

I would like to express my profound gratitude to my friends Sankaranarayanan Padhmanabhan Kavaseri, Sandeep Krishnan, Arun Hejamady Shenoy, Harish Janardhan Bangera, Ramnath Ranganathan, Sreeraj Menon, Prajeeb Kumar Thayyilkumaran, Sharmila Rajendran, Aniket Patankar, Vijay Kalpati, Rahul Rao, Dr. Salah Mehdi and all the other people that do not wish to have their names mentioned.

I would like to thank Jerry Dale, Rodney (Rod) Brakhage and Ron Markum for helping in constructing the experimental setup that I worked on. I would like to thank the MAE staff for their timely help.

I would like to thank the Technical support staff at FIFE corp. and Computer tech. support for their help in my experimental setup.

## TABLE OF CONTENTS

Chapter	Page
<b>1 INTRODUCTION</b>	<b>1</b>
1.1 Background . . . . .	1
1.2 Literature Review . . . . .	2
1.3 The role of dancer rollers in the attenuation of tension variations . . . . .	3
1.3.1 The Passive dancer system . . . . .	4
1.3.2 The active dancer system . . . . .	4
1.4 Thesis Contributions . . . . .	5
1.5 Thesis outline . . . . .	5
<b>2 DYNAMIC EQUATIONS AND SYSTEM IDENTIFICATION</b>	<b>6</b>
2.1 The Active Dancer System . . . . .	9
2.2 The Passive Dancer System . . . . .	13
2.2.1 Dynamic Equations . . . . .	13
2.2.2 Gas Springs . . . . .	18
2.2.3 Mathematical modeling of passive dancer using the gas spring approach . . . . .	20
2.3 Controllers for Active Dancer . . . . .	23
2.3.1 PID controllers . . . . .	23
2.3.2 Internal model controller (IMC) . . . . .	23
<b>3 EXPERIMENTAL WEB PLATFORM</b>	<b>25</b>
3.1 Controller Specifications . . . . .	27

3.1.1	The Data Acquisition Board: DS1103 board . . . . .	28
3.1.2	The dSPACE software . . . . .	28
3.1.3	Optional software packages . . . . .	29
3.1.4	Program files for running the experiments . . . . .	29
3.2	Web guiding systems . . . . .	30
3.2.1	Remotely Pivoted Guide (Kamberoller) . . . . .	31
3.2.2	Offset Pivot Guide (OPG) . . . . .	32
3.2.3	The RPG Guide Controller (The A9 Processor) . . . . .	33
3.3	Load cells . . . . .	33
3.3.1	Dancer Load cells . . . . .	34
3.3.2	Downstream Load cells . . . . .	34
3.3.3	Disturbance Load cells . . . . .	34
3.4	Master Speed Roller . . . . .	35
3.4.1	Nip Roller . . . . .	36
3.5	The Idler Rollers . . . . .	38
3.6	Disturbance Injection in the web line . . . . .	38
3.7	Dancers Rollers . . . . .	39
3.7.1	The Passive Dancer . . . . .	39
3.7.2	The Active Dancer . . . . .	41
3.8	Actuators for Active Dancer . . . . .	43
3.8.1	Electro-mechanical Actuator . . . . .	43
3.8.2	The Electro-Hydraulic Actuator . . . . .	43
3.8.3	The CSP-01 Controller . . . . .	46
3.9	Web Materials . . . . .	46
<b>4</b>	<b>EXPERIMENTAL RESULTS AND CONCLUSIONS</b>	<b>48</b>
4.1	Experiments using passive dancer setup . . . . .	48
4.2	Experiments using active dancer setup . . . . .	50

4.3	Conclusions . . . . .	52
<b>5</b>	<b>SUMMARY AND FUTURE WORK</b>	<b>53</b>
5.1	Summary . . . . .	53
5.2	Future Work . . . . .	54
	<b>BIBLIOGRAPHY</b>	<b>55</b>
<b>A</b>	<b>Experiments on Black polythene web</b>	<b>58</b>
<b>B</b>	<b>Experiments on White paper web</b>	<b>67</b>
<b>C</b>	<b>Calibration of sensors</b>	<b>75</b>
C.1	Downstream Load cell calibration . . . . .	75
C.2	Dancer Load cell calibration . . . . .	75
C.3	Disturbance Load cell . . . . .	77
C.4	Tacho-generator . . . . .	78
C.5	Low pass filter . . . . .	79
C.6	Voltage delimiter . . . . .	80
C.7	Thermal Diffusivity . . . . .	81

## LIST OF FIGURES

Figure	Page
2.1 Schematic of a web passing between two rollers . . . . .	7
2.2 Dancer spans: Unstretched and stretched conditions. . . . .	7
2.3 Active dancer system. $T_0$ is the tension disturbance entering the dancer system, $T_2$ is the controlled tension, and the translational velocity of the dancer roller, $\dot{X}_1$ is the control input. . . . .	9
2.4 Interpretation of the effect of span lengths for an active dancer . . . . .	10
2.5 Free-body diagram of passive dancer . . . . .	13
2.6 An interpretation of the action of passive dancer tension control system. . .	17
2.7 A piston cylinder treated as a spring-damper system . . . . .	18
2.8 Magnitude v/s $Pe_\omega$ . . . . .	21
2.9 Phase v/s $Pe_\omega$ . . . . .	21
3.1 Experimental Web Platform . . . . .	26
3.2 Schematic of Experimental Web Platform . . . . .	27
3.3 Computer . . . . .	28
3.4 dSpace Board . . . . .	28
3.5 Remotely Pivoted Guide and Edge Sensor . . . . .	31
3.6 Offset Pivot Guide, edge sensor and Narrowweb DP-01 controller . . . . .	32
3.7 The A9 Controller . . . . .	33
3.8 The downstream load cell . . . . .	35
3.9 Disturbance load cell . . . . .	36
3.10 Master speed roller, nip roller, tacho-generator and its control panel . . . .	37

3.11	Gas tanks for nip roller and passive dancer . . . . .	37
3.12	Schematic and Picture of Disturbance roller . . . . .	38
3.13	Schematic of Passive Dancer mechanism . . . . .	40
3.14	The passive dancer . . . . .	40
3.15	Schematic of Active Dancer . . . . .	42
3.16	Active Dancer with Load cell and Position Sensor . . . . .	42
3.17	The hydraulic actuator . . . . .	44
3.18	The Moog servo-valve . . . . .	44
3.19	The CSP-01 controller . . . . .	45
3.20	The webs used for experiments . . . . .	47
4.1	Plots showing attenuation using passive dancer at 16 psi and 12 psi respectively . . . . .	49
4.2	Plots showing attenuation using active dancer with hydraulic actuator . . . . .	51
A.1	Plots with disturbance attenuation at 100 fpm at 16psi . . . . .	58
A.2	Plots with disturbance attenuation at 200 and 300 fpm at 16psi . . . . .	59
A.3	Plots with disturbance attenuation at 300 and 400 fpm at 16psi . . . . .	60
A.4	Plots with disturbance attenuation at 400 fpm at 16psi . . . . .	61
A.5	Plots with disturbance attenuation at 100 and 200 fpm at 18psi . . . . .	62
A.6	Plots with disturbance attenuation at 300 and 400 fpm at 18psi . . . . .	63
A.7	Plots with disturbance attenuation at 100 and 200 fpm at 20psi . . . . .	64
A.8	Plots with disturbance attenuation at 300 fpm at 20psi . . . . .	65
A.9	Plots with disturbance attenuation at 400 fpm at 20psi . . . . .	66
B.1	Plot with disturbance attenuation at 200 fpm at 12psi . . . . .	67
B.2	Plots with disturbance attenuation at 300 and 400 fpm at 12psi . . . . .	68
B.3	Plots with disturbance attenuation at 100 and 200 fpm at 14psi . . . . .	69
B.4	Plots with disturbance attenuation at 300 and 400 fpm at 14psi . . . . .	70



B.5	Plots with disturbance attenuation at 100 and 200 fpm at 16psi . . . . .	71
B.6	Plots with disturbance attenuation at 300 and 400 fpm at 16psi . . . . .	72
B.7	Plots with disturbance attenuation at 300 and 400 fpm at 18psi . . . . .	73
B.8	Plots with disturbance attenuation at 300 and 400 fpm at 18psi . . . . .	74
C.1	Calibration plots for the Downstream and Dancer load cells respectively . .	76
C.2	Calibration plot of Disturbance load cell . . . . .	77
C.3	Calibration plot of tacho-generator . . . . .	78
C.4	Plot showing Thermal Diffusivity of Air vs. Temperature . . . . .	81

## NOMENCLATURE

$A$	Cross-sectional area of the web
$B_f$	Bearing friction
$E$	Modulus of elasticity
$J$	Polar moment of inertia of the roller
$K_i$	Web span spring constant ( $EA/L_i$ )
$L_i$	Length of the $i$ -th web span
$M$	Mass of the dancer roller
$R$	Radius of a roller
$T_i$	Change in tension from reference
$U$	Dancer translational velocity input
$V_i$	Change in web velocity from reference
$X$	Change in linear displacement of the dancer roller from the reference
$b$	Viscous friction coefficient of the dancer roller
$k$	Spring constant of the spring loading on the dancer mechanism
$t_r$	Reference web tension
$v_r$	Reference web velocity
$K_p$	Proportional gain
$K_i$	Integral gain
$K_d$	Derivative gain
$K_{imc}$	Gain for the IMC controller

# CHAPTER 1

## INTRODUCTION

### 1.1 Background

The term 'web' is used to describe materials that are manufactured and processed in continuous, flexible strip form, which is very long compared to its width and very wide compared to its thickness. Web materials cover a broad spectrum from extremely thin plastics to paper, textiles, metals, and composites.

Web handling and processing pervades almost every industry today. Web handling involves unwinding material, feeding it to a processing plant and winding it back into a roll after processing. It is essential that the web follow a predetermined path amidst rollers in a longitudinal (along its length) direction at a constant velocity and at a constant tension. Deviation from this may result in an inferior product quality that may be detrimental to further processing and the resulting product.

With the need for increased productivity and performance in the web processing industry, accurate modeling and effective controller design for web handling systems are essential for increasing the processing speed and the quality of the processed web. It is important to maintain web tension within the desired limits under a wide range of dynamic conditions like speed changes, variations in roll sizes, web properties and irregularities. Tension variations beyond certain tolerance levels affect processes and causes damage to the web. This can result in wrinkles and may even lead to breakage of the web. The two main types of tensions that need to be maintained closely are the longitudinal tension and the lateral tension. This report is based mainly on controlling the longitudinal tension.

The reasons for variations in longitudinal tension can be numerous. These can be cate-

gorized into two main types. The disturbances that have their sources external to the system and those that are due to the noise signal in the process itself. Some of these disturbances are periodic in nature (they repeat at regular intervals) and others aperiodic. This thesis concentrates on the periodic type of disturbances (mainly sinusoidal disturbances).

## 1.2 Literature Review

There has been a considerable amount of work done on the attenuation or rejection of tension disturbances. Attenuation of tension disturbances entering the process section is an important aspect in printing and converting industry. The ever increasing range of substrates used in today's packaging industry emphasizes the need for accurate tension control. Controlling tension within a tight tolerance zone is essential for precise registration between the tool and the product in printing and converting machines. A commonly used tension control strategy is to measure the tension in a span upstream to the process section and use this signal as a feedback for the drive motor. Early development of mathematical models for longitudinal dynamics of a web can be found in [1–4]. An overview of lateral and longitudinal dynamic behavior and control of moving webs was presented in [5]. A review of the problems in tension control of webs can be found in [6].

Considerations in the selection of a dancer roller or load cell based tension control approach are discussed in [7–9]. The dancer subsystem may be used as a tension measurement device or as a device to attenuate tension disturbances [10]. When the dancer subsystem is used as a tension measurement device, the displacement of the dancer roller is measured and the tension in the span is inferred from the measured displacement. In contrast, when the dancer subsystem used as a device for attenuating tension disturbances, the dancer subsystem is designed to absorb tension variations. In an active dancer, an actuator is used to control the translational velocity of the dancer roller based on the tension measured by a load cell mounted on a roller downstream to the dancer roller. It is expected that an active dancer will offer a control engineer with an additional flexibility in controlling

tension within tighter tolerance zones [11–15].

### **1.3 The role of dancer rollers in the attenuation of tension variations**

The complex kind of disturbances that are experienced by the web processing lines may be considered to be constituted of basic disturbances and can be categorized as follows,

- Step disturbance
- Ramp disturbance
- Sinusoidal disturbance

As mentioned earlier, the disturbances may be a combination of two or all three of the above. Sinusoidal disturbances themselves can be composed of multiple ones of different frequencies and amplitudes.

Generally a disturbance can be compensated by controlling the speed of the unwind, rewind or the master speed driven roller. If there is a sinusoidal disturbance having a low frequency and amplitude, the above three may provide satisfactory attenuation. In all other cases where high frequency disturbances beyond their scope are encountered, there has to be a more efficient control strategy to attenuate them.

This is where the dancer rollers come into consideration. A dancer roller mechanism is constituted of a web roller which is either connected to a fixed support using passive elements like springs and dampers or is force loaded in opposition to web tension. Irrespective of the loading, the dancer rollers are free to oscillate in one direction and based on their degree of freedom, they are classified into translational and rotational dancers. The criteria for choosing the type of dancers may be a space constraint or a process constraint.

Dancers are commonly used to attenuate tension disturbances caused by uneven rolls, eccentric rolls, misalignment of idler rollers, and periodic slacks in webs. A dancer mechanism may also be used as a feedback in a number of web tension control systems. This

system is driven by the variation in the position of the dancer mechanism in addition to the variations in the actual tension from the desired tension.

### **1.3.1 The Passive dancer system**

The aforementioned type of dancers, that are loaded with springs and dampers, are also called passive dancers on account of the fact that they are composed of passive elements and lack actuators. Passive dancers can be further divided into two categories, viz. dancer rollers with passive elements such as springs and dampers and inertia compensated dancer rollers. Passive dancers are known to act as good tension feedback elements and tension disturbance attenuators for low speed web lines. They have been seen to have limitations in dealing with a wide range of dynamic conditions and resonance problems. In inertia compensated passive dancers, the resonant frequency of the dancer roller is mainly determined by the mass. Thus to increase the frequency range of the tension disturbance that can be attenuated, the dancer roller mass must be changed. However, the weight of the dancer roller needs to be twice the reference web tension, which limits any changes to the dancer roller mass to increase the resonant frequency.

### **1.3.2 The active dancer system**

It is seen that by introducing an active element into a dancer mechanism, more control and flexibility is obtained in attenuating periodic tension disturbances and over a wider range of frequencies. An active dancer, effectively, is a passive dancer with the actuator added to improve its response characteristics. The measure of this improvement is indicated by the increase in bandwidth in the frequency response plot. The dancer can respond to higher frequencies of fluctuations in tension thus overcoming the limitation posed by the passive dancer system.

The focus of this thesis is on modeling and experimental evaluation of a passive dancer system and an active dancer system for attenuation of periodic disturbance in tension.

## **1.4 Thesis Contributions**

The contributions of this thesis can be summarized as follows.

- A detailed investigation of how much attenuation can be achieved using a passive and an active dancer system is made for the web handling system under consideration.
- A system identification for the passive dancer is made on the basis of the concept of gas springs. A model is proposed.
- One controller is selected to be the best out of the two controllers designed and future direction of research is suggested.

## **1.5 Thesis outline**

This report is organized as follows.

- The system dynamics and the dynamics of the dancer systems under consideration are discussed in chapter 2.
- System identification for the passive dancer system with a gas spring is discussed in chapter 2.
- A detailed description of the traction machine and its components, and a preview of its computer and controllers is given in chapter 3.
- The results of the experiments run using the passive dancer mechanism for disturbance attenuation, based on various factors is presented and conclusions are drawn in chapter 4.
- The summary of the whole thesis in chapter 5.

## CHAPTER 2

### DYNAMIC EQUATIONS AND SYSTEM IDENTIFICATION

A web handling system is a dynamic system for a few reasons, some of which are listed below.

- There are rollers that are in constant rotational and occasionally translational motion. Their inertia and dynamic friction come into play during web handling.
- There are operations that the web passes through such as printing, cutting, embossing etc. that add their own dynamics and disturbances.
- The web itself has some inherent elastic properties and there are dynamics associated with this elasticity.
- There are noise signals due to electric or magnetic fields around the web machine that could affect the actuators.

These dynamics create problems like web deformations, wrinkling and breaking, that are undesirable. In order to have efficient web handling, these factors have to be acknowledged and dealt with appropriately.

The web tension and the web velocity are the two major variables of concern, and these affect each other, in a very complicated fashion. The equations that relate the two are non-linear and at higher speeds this dynamics becomes more prominent.

Consider the web shown in the figure 2.1, passing through the two rollers and moving towards the right. Here  $\varepsilon_{iv}$  denotes the strain in the  $i^{th}$  web span due to velocity variations. It is assumed as a convention that the  $i^{th}$  web span precedes the  $i$ th roller. In dancer systems,



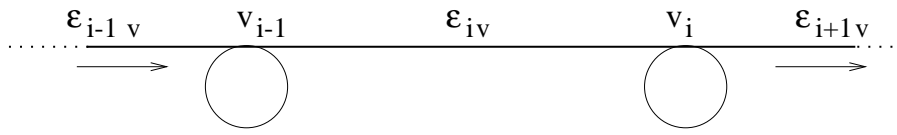


Figure 2.1: Schematic of a web passing between two rollers

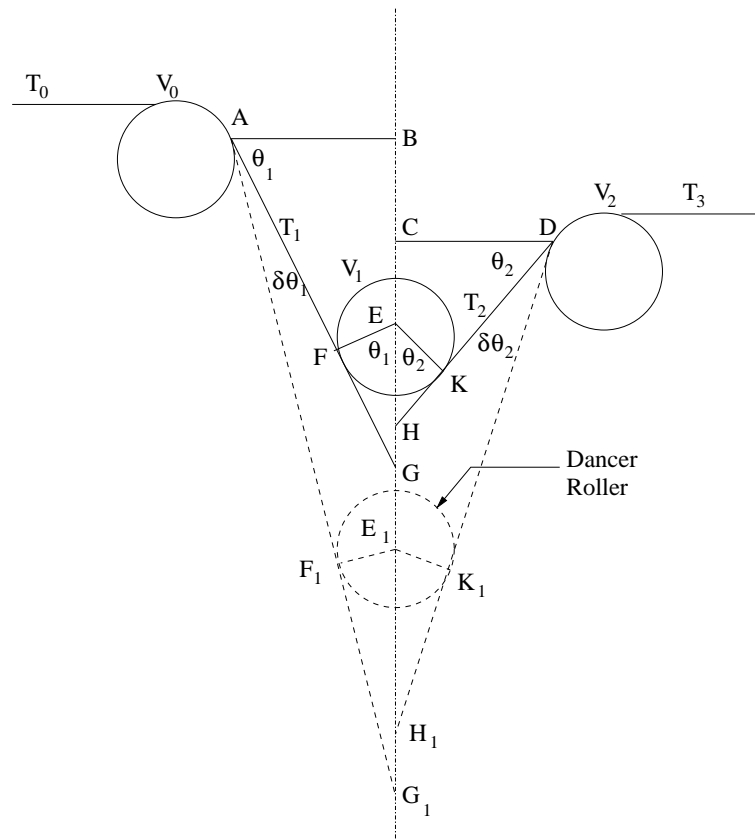


Figure 2.2: Dancer spans: Unstretched and stretched conditions.

the strain in web spans adjacent to the dancer roller is due to web velocity variations and the dancer roller translational movements.

The dynamics that comes into play while the web is in motion, is governed by an equation given by,

$$L_i \frac{d}{d\tau} \varepsilon_{iv} = v_i - v_i \varepsilon_{iv} - v_{i-1} \varepsilon_{(i-1)v}. \quad (2.1)$$

The web span dynamics and the fact that the net strain in the web upstream and downstream to the dancer roller is the sum of the strains due to the web velocity variation and the dancer movements, is used to derive the tension dynamics.

Under the assumption that the web is elastic we know that

$$\varepsilon_i = \frac{T_i}{EA}. \quad (2.2)$$

The material may be considered to be viscoelastic, in which case the tension in the web will be given by

$$T_i = EA\varepsilon_i + bL\dot{\varepsilon}_i. \quad (2.3)$$

In this thesis the expression is derived only for the elastic web. The following linearized expression can be obtained for the spans shown in the figure 2.2.

$$L_2 \dot{t}_2 = EA(v_2 - v_1) + (v_1 t_1 - v_2 t_2) + \left( \frac{v_2}{L_2 \sin \theta_1} - \frac{v_2}{L_2 \sin \theta_1} \right) EAx + EA \frac{\dot{x}}{\sin \theta_2}, \quad (2.4)$$

$$L_1 \dot{t}_1 = EA(v_1 - v_0) + (v_0 t_0 - v_1 t_1) + \left( \frac{EA v_1 x}{L_1 \sin \theta_1} \right) + EA \frac{\dot{x}}{\sin \theta_1} \quad (2.5)$$

Equations 2.4 and 2.5 are nonlinear involving terms such as  $v_i t_i$ . To obtain linearized equations around given reference values of web velocity ( $v_r$ ), web tension ( $t_r$ ), and dancer displacement ( $x_r = 0$ ), let  $V_i = v_i - v_r$ ,  $T_i = t_i - t_r$ , and  $X = x$  represent the deviations. Substituting into equations (2.4) and (2.5), we obtain the linearized dynamics of web spans upstream and downstream to the dancer roller as

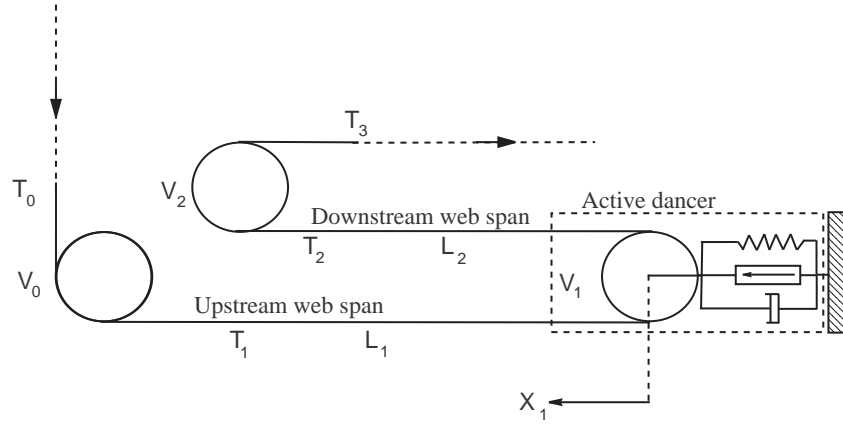


Figure 2.3: Active dancer system.  $T_0$  is the tension disturbance entering the dancer system,  $T_2$  is the controlled tension, and the translational velocity of the dancer roller,  $\dot{X}_1$  is the control input.

$$L_1 \dot{T}_1 = (EA - t_r)(V_1 - V_0) + v_r(T_0 - T_1) + \frac{EA}{L_1 \sin \theta_1} v_r X + \frac{EA \dot{X}}{\sin \theta_1} \quad (2.6)$$

$$L_2 \dot{T}_2 = (EA - t_r)(V_2 - V_1) + v_r(T_1 - T_2) + EA v_r \left( \frac{1}{L_2 \sin \theta_2} - \frac{1}{L_1 \sin \theta_1} \right) + \frac{EA \dot{X}}{\sin \theta_2} \quad (2.7)$$

where

$L_1$  = Initial length of the upstream span

$L_2$  = Initial length of the downstream span

$T_1$  = Tension in the downstream span

$T_2$  = Tension in the upstream span

## 2.1 The Active Dancer System

The web span developed in the previous section was for a general roller which may not be uniform with respect to the adjacent rollers. It is convenient to measure the tension in the spans if the dancer roller is centrally located between the upstream and downstream rollers

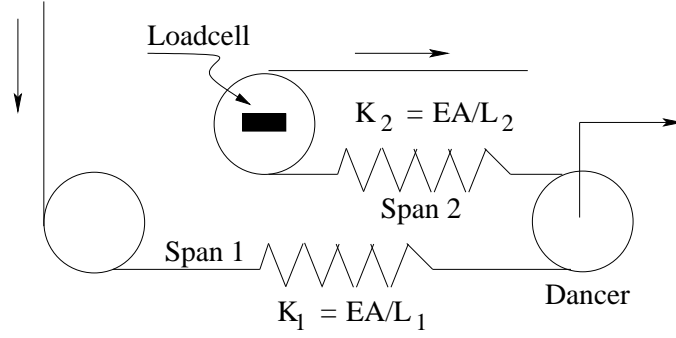


Figure 2.4: Interpretation of the effect of span lengths for an active dancer

and the wrap angle on the dancer roller is 180 degrees, i.e.,  $\theta_1 = \theta_2 = 90$  degrees. Further the angle of wrap remains equal for the normal and stretched conditions of the web spans. The non-linearity of the tension dynamics can thus be reduced in terms of the angle of wrap of the web on the dancer roller. With this observation the active dancer system is considered as in the given figure. This system consists web spans adjacent to the dancer roller in the upstream and downstream directions and the three rollers including the dancer roller. All the variables shown in the schematic represent variations from from their reference values. It is assumed that  $T_0$  is the upstream tension disturbance that needs to be rejected using the active dancer system.

The angular dynamics of each roller is given by,

$$J_i \dot{\omega}_i = -B_{f_i} \omega_i + R_i (t_{i+1} - t_i), \quad (2.8)$$

Assuming that there is no slip of the web on the rollers, the web velocity can be given on each roller as  $v_i = R_i \omega_i$ . Therefore the linearized dynamics of the web velocity on each roller can be given by

$$J_i \dot{V}_i = -B_{f_i} V_i + R_i^2 (T_{i+1} - T_i), \quad (2.9)$$

Using  $\theta_1 = \theta_2 = 90$  degrees in the equations derived in the previous section and assuming that the rollers are identical which means  $J_i = J$  and  $R_i = R$ . The dynamic

equations for the active dancer shown in the schematic are given by

$$\beta\dot{V}_0 = -\gamma V_0 + (T_1 - T_0), \quad (2.10)$$

$$\tau_1\dot{T}_1 = -T_1 + T_0 + \alpha(V_1 - V_0) + \frac{\alpha}{\tau_1}X + \alpha U, \quad (2.11)$$

$$\beta\dot{V}_1 = -\gamma V_1 + (T_2 - T_1), \quad (2.12)$$

$$\tau_2\dot{T}_2 = -T_2 + T_1 + \alpha(V_2 - V_1) + \alpha\left(\frac{1}{\tau_2} - \frac{1}{\tau_1}\right)X + \alpha U, \quad (2.13)$$

$$\beta\dot{V}_2 = -\gamma V_2 + (T_3 - T_2), \quad (2.14)$$

$$\dot{X} = U, \quad (2.15)$$

where  $\beta = \frac{J}{R^2}$ ,  $\gamma = \frac{B_f}{R^2}$ ,  $\alpha = \frac{EA}{v_r}$ ,  $\tau_1 = \frac{L_1}{v_r}$  and  $\tau_2 = \frac{L_2}{v_r}$ .

Since the value of EA is smaller than  $t_r$  for most webs, the  $t_r$  term is neglected in obtaining the above equations from the ones in the earlier section. The input/output model is obtained by assuming that the roller bearing friction is negligible ( $\gamma = B_f/R^2 \approx 0$ ).

It is also assumed that the moment of inertia of all rollers are the same i.e.,  $J_i = J$  and  $R_i = R$  for  $i = 1, 2, 3$ . The input/output model for the active dancer subsystem can be derived by considering the translational velocity of the dancer roller ( $U$ ) as the control input and tension ( $T_2$ ) at the roller immediately downstream of the dancer roller as the measured output. Taking the Laplace transform of equations (2.10)-(2.15) and simplifying, we obtain

$$\mathbf{T}_1(s) = \mathbf{G}_1(s)\mathbf{T}_0(s) + \mathbf{G}_2(s)\mathbf{T}_2(s) + \mathbf{G}_3(s)\mathbf{X}(s) \quad (2.16)$$

$$\mathbf{T}_2(s) = \mathbf{G}_4(s)\mathbf{T}_1(s) + \mathbf{G}_5(s)\mathbf{T}_3(s) + \mathbf{G}_6(s)\mathbf{X}(s) \quad (2.17)$$

where the transfer functions  $\mathbf{G}_1(s)$  through  $\mathbf{G}_6(s)$  are given by the following set of

equations.

$$\mathbf{G}_1(s) = \frac{(\beta s + \gamma + \alpha)}{((\beta s + \gamma)(\tau_1 s + 1) + 2\alpha)} \quad (2.18)$$

$$\mathbf{G}_2(s) = \frac{\alpha}{((\beta s + \gamma)(\tau_1 s + 1) + 2\alpha)} \quad (2.19)$$

$$\mathbf{G}_3(s) = \frac{\alpha(\beta s + \gamma)(s + \varepsilon_1)}{((\beta s + \gamma)(\tau_1 s + 1) + 2\alpha)} \quad (2.20)$$

$$\mathbf{G}_4(s) = \frac{(\beta s + \gamma + \alpha)}{((\beta s + \gamma)(\tau_2 s + 1) + 2\alpha)} \quad (2.21)$$

$$\mathbf{G}_5(s) = \frac{\alpha}{((\beta s + \gamma)(\tau_2 s + 1) + 2\alpha)} \quad (2.22)$$

$$\mathbf{G}_6(s) = \frac{\alpha(\beta s + \gamma)(s + \varepsilon)}{((\beta s + \gamma)(\tau_2 s + 1) + 2\alpha)} \quad (2.23)$$

Substituting the expression for  $\mathbf{T}_1(s)$  from (2.16) into (2.17) and simplifying results in the following input/output model:

$$\mathbf{T}_2(s) = \frac{\mathbf{D}_{ad}(s)}{\mathbf{C}_{ad}(s)} \mathbf{U}(s) + \frac{\mathbf{A}_{ad}(s)}{\mathbf{C}_{ad}(s)} \mathbf{T}_0(s) + \frac{\mathbf{B}_{ad}(s)}{\mathbf{C}_{ad}(s)} \mathbf{T}_3(s), \quad (2.24)$$

where  $\mathcal{L}(T_i(t)) \triangleq \mathbf{T}_i(s)$ ,  $i = 0, 1, 2, 3$ ,  $\mathcal{L}(U(t)) \triangleq \mathbf{U}(s)$ ,  $\eta \triangleq \beta/\alpha$ , and

$$\mathbf{A}_{ad}(s) = (\eta s + 1)^2, \quad (2.25)$$

$$\mathbf{B}_{ad}(s) = \eta s(\tau_1 s + 1) + 2, \quad (2.26)$$

$$\mathbf{C}_{ad}(s) = \eta^2 \tau_1 \tau_2 s^4 + \eta^2 (\tau_1 + \tau_2) s^3 + \eta(\eta + 2\tau_1 + 2\tau_2) s^2 + 3\eta s + 3, \quad (2.27)$$

$$\mathbf{D}_{ad}(s) = \beta \eta \tau_1 s^3 + \beta \eta \left(1 + \frac{\tau_1}{\tau_2}\right) s^2 + \beta \left(3 + \frac{\eta}{\tau_2}\right) s + \beta \left(\frac{2}{\tau_2} - \frac{1}{\tau_1}\right). \quad (2.28)$$

Notice that, if  $\tau_2 > 2\tau_1$ , i.e.,  $L_2 > 2L_1$ , then the constant term of the polynomial  $\mathbf{D}_{ad}(s)$  is negative, which results in a zero in the right-half of the complex plane. This fact forms an important constraint on the implementation of the active dancer, which will be discussed later.

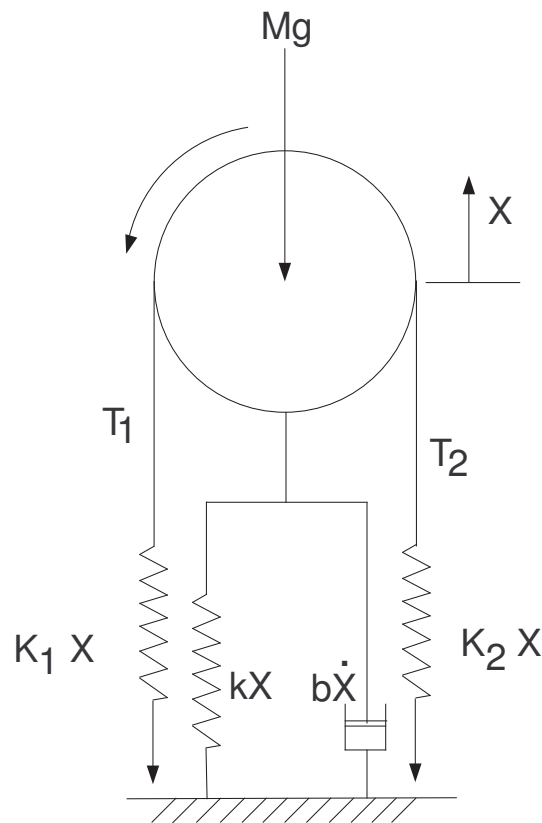


Figure 2.5: Free-body diagram of passive dancer

## 2.2 The Passive Dancer System

The passive dancer can be treated as an active dancer without the actuator. It is supposed to have a mass, spring and damper to effect attenuation.

### 2.2.1 Dynamic Equations

In this section, a complete model of the passive dancer followed by a simplified model is presented; the simplified model will be used to analyze the action of the passive dancer in rejecting web tension disturbances.

As a first step, notice that if the dancer roller is passive (that is, no external actuator is used to position the dancer roller,  $F = 0$ ; see Fig. 2.5), the equation governing the

dynamics of the dancer roller is given by

$$m\ddot{X} + b\dot{X} + kX = T_1(t) + T_2(t). \quad (2.29)$$

Taking the Laplace transform of the above equation results in

$$\mathbf{X}(s) = \frac{1}{(Ms^2 + bs + k)} [\mathbf{T}_1(s) + \mathbf{T}_2(s)] \quad (2.30)$$

It may be noticed here that equations (2.16) and (2.17) are applicable for the case of passive dancer also; in the case of the active dancer  $\mathbf{X}(s)$  in equations (2.16) and (2.17) is controlled independently by an actuator, whereas, for the passive dancer  $\mathbf{X}(s)$  is given by (2.30). Define  $\bar{b}$ ,  $\bar{k}$  and  $\bar{\beta}$  as

$$\bar{b} = \frac{b}{M}, \quad \bar{k} = \frac{k}{M} \quad \text{and} \quad \bar{\beta} = \frac{\beta}{M}.$$

Substituting (2.30) into (2.16) and (2.17) and simplifying, we obtain

$$\mathbf{T}_1(s) = \mathbf{H}_1(s)\mathbf{T}_0(s) + \mathbf{H}_2(s)\mathbf{T}_2(s) \quad (2.31)$$

$$\mathbf{T}_2(s) = \mathbf{H}_3(s)\mathbf{T}_1(s) + \mathbf{H}_4(s)\mathbf{T}_3(s) \quad (2.32)$$

where the transfer functions  $\mathbf{H}_1(s)$  through  $\mathbf{H}_4(s)$  are given in the following set of equations.

$$\mathbf{H}_1(s) = \frac{(\eta s + 1)(s^2 + \bar{b}s + \bar{k})}{((\eta s(\tau_1 s + 1) + 2)(s^2 + \bar{b}s + \bar{k}) - \bar{\beta}s(s + \varepsilon_1))} \quad (2.33)$$

$$\mathbf{H}_2(s) = \frac{(s^2 + \bar{b}s + \bar{k}) - \bar{\beta}s(s + \varepsilon_1)}{((\eta s(\tau_1 s + 1) + 2)(s^2 + \bar{b}s + \bar{k}) - \bar{\beta}s(s + \varepsilon_1))} \quad (2.34)$$

$$\mathbf{H}_3(s) = \frac{(\eta s + 1)(s^2 + \bar{b}s + \bar{k}) + \bar{\beta}s(s + \varepsilon)}{((\eta s(\tau_2 s + 1) + 2)(s^2 + \bar{b}s + \bar{k}) - \bar{\beta}s(s + \varepsilon))} \quad (2.35)$$

$$\mathbf{H}_4(s) = \frac{(s^2 + \bar{b}s + \bar{k})}{((\eta s(\tau_2 s + 1) + 2)(s^2 + \bar{b}s + \bar{k}) - \bar{\beta}s(s + \varepsilon))} \quad (2.36)$$

Substituting the expression for  $\mathbf{T}_1(s)$  given by (2.31) into (2.32) we obtain

$$\mathbf{T}_2(s) = \frac{\mathbf{A}_{pd}(s)}{\mathbf{C}_{pd}(s)}\mathbf{T}_0(s) + \frac{\mathbf{B}_{pd}(s)}{\mathbf{C}_{pd}(s)}\mathbf{T}_3(s) \quad (2.37)$$



where

$$\mathbf{A}_{pd}(s) = \left[ (\eta s + 1) (s^2 + \bar{b}s + \bar{k}) - \bar{\beta}s \left( s + \frac{1}{\tau_2} - \frac{1}{\tau_1} \right) \right] (\eta s + 1) (s^2 + \bar{b}s + \bar{k}) \quad (2.38)$$

$$\mathbf{B}_{pd}(s) = (s^2 + \bar{b}s + \bar{k}) \left[ (\eta s (\tau_1 s + 1) + 2) (s^2 + \bar{b}s + \bar{k}) - \bar{\beta}s \left( s + \frac{1}{\tau_1} \right) \right] \quad (2.39)$$

$$\begin{aligned} \mathbf{C}_{pd}(s) = & \left[ (\eta s (\tau_1 s + 1) + 2) (s^2 + \bar{b}s + \bar{k}) - \bar{\beta}s \left( s + \frac{1}{\tau_1} \right) \right] \\ & \times \left[ (\eta s + 1) (s^2 + \bar{b}s + \bar{k}) - \bar{\beta}s \left( s + \frac{1}{\tau_2} - \frac{1}{\tau_1} \right) \right] \\ & - \left[ (s^2 + \bar{b}s + \bar{k}) - \bar{\beta}s \left( s + \frac{1}{\tau_1} \right) \right] \left[ (\eta s + 1) (s^2 + \bar{b}s + \bar{k}) - \bar{\beta}s \left( s + \frac{1}{\tau_2} - \frac{1}{\tau_1} \right) \right] \end{aligned} \quad (2.40)$$

where

$$\bar{b} = \frac{b}{M}, \quad \bar{k} = \frac{k}{M} \quad \text{and} \quad \bar{\beta} = \frac{\beta}{M}$$

The coefficients of the polynomial  $A_{pd}(s)$ ,  $B_{pd}(s)$  and  $C_{pd}(s)$  depend on the mechanical features of the dancers and the properties of the web material. This, in turn, indicates that, in the case of a passive dancer, the behavior of the tension  $T_2$  is solely determined by the mechanical features of the passive dancer (the mass of the dancer roller  $M$ , the spring constant  $k$ , and the viscous friction constant  $b$ ), and the properties of the web material (Young's modulus  $E$  and the cross-sectional area of the web  $A$ ).

Equations (2.24) and (2.37) are similar in structure except for the term involving the dancer velocity input,  $\mathbf{U}(s)$ , in the active dancer input/output model. It is important to note that setting  $\mathbf{U}(s) = 0$  in the active dancer input/output model will not make the equations (2.24) and (2.37) identical. Since  $\mathbf{U}(s)$  is the dancer translational velocity, setting  $\mathbf{U}(s) = 0$  would mean that the dancer roller is arrested at a particular position and thus acts as an idle roller.

Though the linearized model of the passive dancer, presented in equation (2.37), is a fairly accurate model, it is not clear as to how one would conduct analysis to highlight the characteristics of the passive dancer using this model. In specific, the dynamics of the passive dancer is characterized by six independent parameters, *viz.*,  $\bar{b}$ ,  $\bar{k}$ ,  $\bar{\beta}$ ,  $\tau_1$ ,  $\tau_2$ ,

and  $\eta$ . Thus, to analyze the system using classical techniques, such as frequency response technique, each combination of the six parameters need to be considered to arrive at meaningful conclusions about the performance of the dancer. Such an analysis is cumbersome and overwhelming. To bring out the inherent features of the passive dancer, a simple, intuitive explanation of the passive dancer is needed. Consequently, to illustrate the tension disturbance attenuation features of the passive dancer, we will develop a simplified model of the passive dancer in the following.

Figure 2.5 shows a free-body diagram of the passive dancer roller. Assuming that the web is mostly elastic and obeys Hooke's law, the spans adjacent to the passive dancer can be represented as springs with stiffness  $K_1$  and  $K_2$  respectively;  $K_1 = EA/L_1$  and  $K_2 = EA/L_2$ . The net tension in span 1 is the sum of the spring force due to dancer displacement,  $K_1X$ , and any disturbance,  $d_1$ , entering the span, so  $t_1 = K_1X + d_1$ . Similarly,  $t_2 = K_2X + d_2$ . Notice that if the material of the web is visco-elastic, then the force in the span may be modeled as  $K_1X + B_v\dot{X}$  where the damping  $B_v$  reflects the viscosity of the web material.

The effect of the air pressure is modeled as a spring force  $kX$  and a damping force  $b\dot{X}$ . From the free-body diagram, the equation of motion of the passive dancer is obtained by a force balance in the vertical direction as

$$\begin{aligned}
 M\ddot{X} + b\dot{X} + kX &= Mg + e, \\
 e &\triangleq t_1 + t_2 = (K_1 + K_2)X + w, \\
 w &\triangleq d_1 + d_2.
 \end{aligned}
 \tag{2.41}$$

The reference value of  $e$  is obtained as the sum of tensions  $t_1$  and  $t_2$  at the reference point:  $e_r = t_r + t_r = 2t_r$ . To analyze equation (2.41), we represent it by a control block diagram shown in Fig. 2.6, where  $w$  denotes the tension disturbance and  $X$  denotes the displacement of the passive dancer roller around the equilibrium point.

Equilibrium point here means that the position of the dancer roller when there are no disturbances, that is, when  $w(t)=0$ . The tension variation around the equilibrium point is

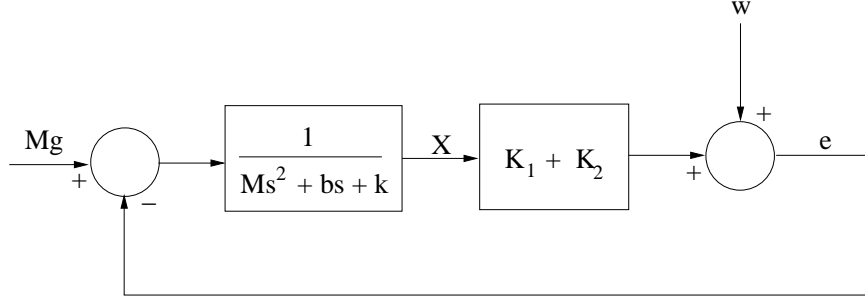


Figure 2.6: An interpretation of the action of passive dancer tension control system.

given by

$$E(t) \triangleq e - e_r = t_1 + t_2 - 2t_r = (t_1 - t_r) + (t_2 - t_r) = T_1(t) + T_2(t).$$

The passive dancer attempts to offer a reaction force to minimize  $E(t)$  whenever disturbance  $w(t)$  appears. From the block diagram, and using equations (2.41), we may write,

$$\mathbf{E}(s) = \underbrace{\frac{Ms^2 + bs + k}{Ms^2 + bs + k - (K_1 + K_2)}}_{\mathbf{G}_{passive}(s)} \mathbf{W}(s) - \underbrace{\frac{K_1 + K_2}{Ms^2 + bs + k - (K_1 + K_2)}}_{\mathbf{G}_{mass}(s)} Mg \quad (2.42)$$

where  $\mathbf{E}(s) \triangleq \mathcal{L}(e(t))$  and  $\mathbf{W}(s) \triangleq \mathcal{L}(w(t))$  are the Laplace transforms of  $e(t)$  and  $w(t)$ , respectively. Equation (2.42) characterizes the control action of the passive dancer for tension disturbance attenuation and highlights many important features of the passive dancer. The next section compares passive and active dancers.

Note that in the absence of a disturbance signal,  $w$ , the tensions would remain constant and the sum of tensions,  $e$ , can be obtained by equating the terms with the laplace coefficients  $s$  to zero.

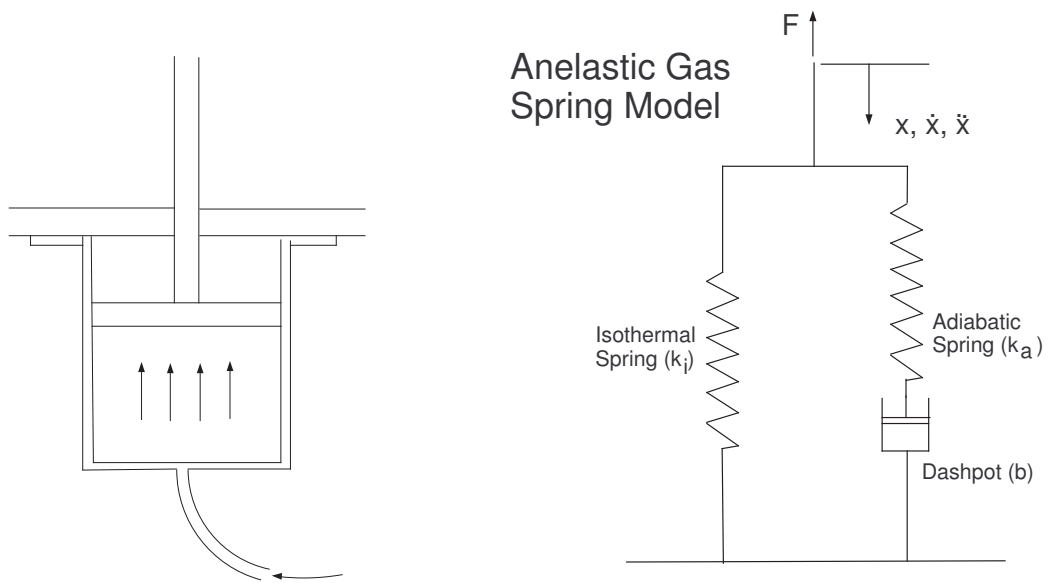


Figure 2.7: A piston cylinder treated as a spring-damper system

### 2.2.2 Gas Springs

The dynamic element that the passive dancer system functions on is a piston-cylinder arrangement. The cylinder is pressurized with air and the piston is loaded with the carriage that carries the roller. The carriage has a significant mass and in this case it is added to the varying web tension that also acts downwards. This passive element can be treated as a gas spring that offers a combined effect of a spring and a damper.

The characteristic properties of air and piston-cylinders that are pertinent to the behavior of this system are given below.

- Gas thermal Diffusivity ( $\alpha$ ).
- Gas specific heat ratio ( $\gamma$ ).
- Volume (V).
- Pressure (P).
- Hydraulic diameter: Same as bore diameter for circular cylinders ( $D_h$ ).

- Piston area (A).

Gas springs are used to provide a force varying with displacement as do conventional springs, except that the elasticity is acquired using the compressibility of a gas. In this thesis air is used as the compressible gas. Like conventional springs, the gas springs exhibit

- A force-distance amplitude relationship.
- A phase shift between the force and the distance that varies with frequency.
- Dissipation of heat energy as a result of the phase shift between force and distance.

In case of conventional springs, there is a region of operation where the spring exhibits linear dynamics. The gas springs, however, are nonlinear throughout their range of operation. This is because their compressibility is dependent on many factors like pressure, control volume, temperature and the characteristics of gas used. Despite this inherent non-linearity, they have an advantage over conventional springs; the properties of the spring can be varied only by changing one of the aforementioned factors. The overall mechanical setup may stay unaltered. Moreover the type of gas used can be either monatomic or diatomic, depending on the dynamics required. Air, in this case, can be considered to be diatomic based on its specific heat ratio ( $\gamma$ ).

Due to the inherent nonlinearity, there are linearized models that can be used for running simulation and experiments. While linearized models can only approximate the performance of the actual model, it is desirable to use the best available linear model. The model proposed by A. A. Kornhauser (1994) is used in this thesis for modeling the gas spring.

The schematic and the free body diagram of the gas spring is shown in figure 2.2.2. The values of isothermal spring constant  $k_i$  and adiabatic constant  $k_a$  are calculated using,

$$k_i = \frac{A^2 P_0}{V_0} \quad \text{and} \quad k_a = (\gamma - 1) \frac{A^2 P_0}{V_0} \quad (2.43)$$

The differential equation for the anelastic model is given by,

$$F - F_0 + \frac{b}{k_a} \dot{F} = k_i (x - x_0) + b \left( 1 + \frac{k_i}{k_a} \right) \dot{x} \quad (2.44)$$

The input displacement to the system is a sinusoid given by  $x = x_0 + x_a \sin \omega t$ . The resulting force has a magnitude and phase with respect to the input that is given by

$$\begin{aligned} \hat{F} &= \frac{|F|}{x_a (k_i + k_a)} \\ &= \frac{1}{k_i + k_a} \sqrt{\frac{k_i^2 k_a^2 + b^2 \omega^2 (k_i + k_a)^2}{k_a^2 + b^2 \omega^2}} \end{aligned} \quad (2.45)$$

$$\phi = \arctan \left[ \frac{b \omega k_a^2}{k_i^2 k_a + b^2 \omega^2 (k_i + k_a)} \right] \quad (2.46)$$

These values of  $k_a$  and  $k_i$  can be combined further to a non-dimensional value  $\hat{K}$ .

$$\hat{K} = \frac{k_i}{k_a} = \frac{1}{\gamma - 1} \quad (2.47)$$

Value of  $\hat{K}$  is 2.5 for air. Similarly a non-dimensional damping coefficient can be introduced.

$$\hat{B} = \frac{4\alpha b}{k_a D_h^2} = \frac{b\omega}{k_a Pe_\omega} \quad (2.48)$$

where  $Pe_\omega$  is Peclet's number. The magnitude and phase equations can be rewritten as follows.

$$\hat{F} = \frac{1}{\hat{K} + 1} \sqrt{\frac{\hat{K}^2 + \hat{B}^2 Pe_\omega^2 (\hat{K} + 1)^2}{1 + \hat{B}^2 Pe_\omega^2}} \quad (2.49)$$

$$\phi = \arctan \left[ \frac{\hat{B} Pe_\omega}{\hat{K} + \hat{K} \hat{B}^2 Pe_\omega^2 + \hat{B}^2 Pe_\omega^2} \right] \quad (2.50)$$

The plots for the magnitude and phase of the resultant force are shown in figures 2.8 and 2.9.

### 2.2.3 Mathematical modeling of passive dancer using the gas spring approach

The difference between the gas spring system discussed earlier and the system under consideration is that the mass of the carriage is considered to be significant. Hence the differ-

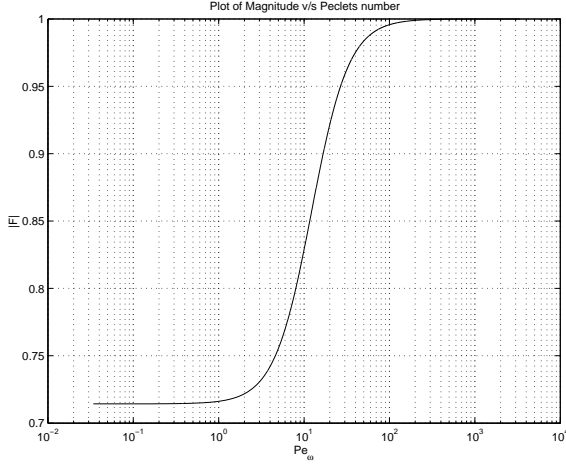


Figure 2.8: Magnitude v/s  $Pe_\omega$

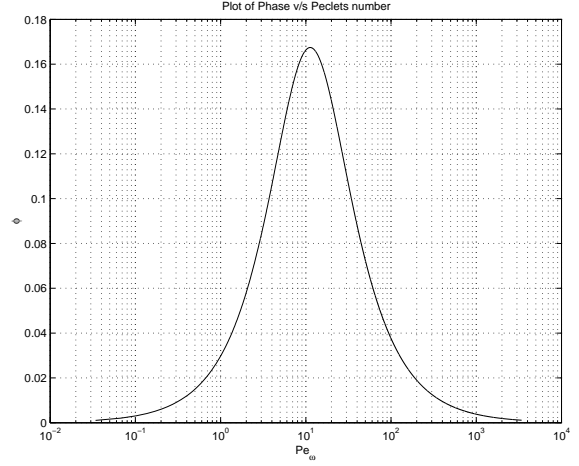


Figure 2.9: Phase v/s  $Pe_\omega$

ential equation that is derived earlier is modified to the following form.

$$F - F_0 + \frac{b}{k_a} \dot{F} = k_i (x - x_0) + b \left( 1 + \frac{k_i}{k_a} \right) \dot{x} + m\ddot{x} \quad (2.51)$$

Taking laplace transforms on both sides of the equation, we obtain the following equation.

$$F(s) + \frac{b}{k_a} [sF(s) - f(0)] = k_i X(s) + b \left( 1 + \frac{k_i}{k_a} \right) [sX(s) - x(0)] + m [s^2 X(s) - sx(0) - \dot{x}(0)] \quad (2.52)$$

$$F(s) \left[ 1 + \frac{b}{k_a} s \right] - \frac{b}{k_a} F_0 = \left[ k_i + b \left( 1 + \frac{k_i}{k_a} \right) s + ms^2 \right] X(s) - \left[ b \left( 1 + \frac{k_i}{k_a} \right) - ms \right] x(0) - m\dot{x}(0) \quad (2.53)$$

Considering the initial position and velocity of the dancer to be zero, and the initial force to be zero as well, we can obtain the transfer function in the Laplace domain as,

$$\frac{X(s)}{F(s)} = \left[ \frac{\frac{b}{k_a} s + 1}{ms^2 + b \left( 1 + \frac{k_i}{k_a} \right) s + k_i} \right] \quad (2.54)$$

The parameters in the above transfer function can be calculated as using the expressions

that follow.

$$m = 15.5 \text{ lbs (mass of passive dancer carriage)}$$

$$b = \frac{\hat{B}k_a D_h^2}{4\alpha}$$

$$k_a = \frac{A^2 P_0}{V_0}$$

$$k_i = \frac{(\gamma - 1)A^2 P_0}{V_0}$$

where

$$\hat{B} = 0.072 \text{ (for diatomic gases)}$$

$D_h$  = Hydraulic diameter of the cylinder

$\alpha$  = Thermal diffusivity obtained for air from the plot

$P_0$  = 12, 14, 16, 18 or 20 *psi*

$V_0$  = Total volume of the cylinder, buffer tank and the tube

$A$  = Area of cross-section of cylinder =  $\frac{\pi}{4}d^2$

$d$  = diameter of the cylinder.



## 2.3 Controllers for Active Dancer

The controllers that were implemented for disturbance rejection using active dancers, were the PID and the IMC controllers. These were chosen because the mathematical model of the active dancer mechanism with the hydraulic actuator was not known.

### 2.3.1 PID controllers

A PID controller can be written mathematically in the continuous time domain as

$$u(t) = K_p e(t) + K_i \int_0^t e(\tau) d\tau + K_d \frac{de(t)}{dt} \quad (2.55)$$

$$U(s) = \left( K_p + \frac{K_i}{s} + K_d s \right) E(s) \quad (2.56)$$

where  $u(t)$  is the control input to the plant and  $e(t)$  is the feedback error signal. The gains  $K_p$ ,  $K_d$  and  $K_i$  are chosen appropriately to achieve the desired behavior.

The discrete time version of the PID controller can be written as

$$u(k) = K_p e(k) + K_i T_s \sum_{j=1}^k e(j) + K_d \left( \frac{e(k) - e(k-1)}{T_s} \right) \quad (2.57)$$

$$U(z) = \left( K_p + K_i \frac{T_s z}{z-1} + \frac{K_d (z-1)}{T_s z} \right) E(z) \quad (2.58)$$

### 2.3.2 Internal model controller (IMC)

In this type of controller, the internal model of the disturbance, if known, is used for calculating the parameters and gains for the controller. This type of controllers are useful when some information is available regarding the disturbance (especially the periodicity/frequency).

In this case the periodic disturbance is of the form

$$d(t) = A \sin(\omega t + \phi) \quad (2.59)$$

Here  $A$  and  $\phi$  may be unknown but if  $\omega$  is known, an internal model controller can be designed in the form

$$G_c(z) = K_p + \frac{z^{-1}K_{imc} \sin(\omega T_s)}{1 - 2z^{-1} \cos(\omega T_s) + z^{-2}} \quad (2.60)$$

The Proportional gain  $K_p$  takes care of the absolute mean of the disturbance and the IMC gain,  $K_{imc}$  is used to reject the amplitude of the disturbance.

Effectively the controller tries to negate the effect of the disturbance by introducing a signal of the same type. There may be a phase difference between the controller sinusoid and the disturbance, but that can be compensated by a PI controller for the phase embedded in the IMC controller.

In this case, the disturbance is injected using an eccentric roller, driven by the web. If the slip between the roller and the web is negligible, then the angular velocity of the roller is proportional to the linear velocity of the web. The frequency of disturbance can be easily measured by using a tachogenerator on the eccentric roller, or on the master-speed motor.

The discrete time version of the IMC controller is given by,

$$\begin{aligned} U(k) = & K_p E(k) + E(k-1) [K_{imc} \sin(\omega T_s) - 2K_p \cos(\omega T_s)] \\ & + K_p E(k-2) + 2U(k-1) \cos(\omega T_s) - U(k-2) \end{aligned} \quad (2.61)$$

where  $U(k)$  is the control input to the active dancer in a real-time implementation.

## CHAPTER 3

### EXPERIMENTAL WEB PLATFORM

The experiments for this thesis are run on an experimental web platform. The figure 3.2 shows the schematic of the experimental machine with the passive dancer and the active dancer.

The figure 3.1 shows a picture of the actual experimental web platform that is used to run all the experiments. A schematic representation of the same is shown in figure 3.2.

The platform primarily consists of an endless web line with many rollers, a couple of web guides for maintaining lateral position of the web and a couple of dancers, viz., an active dancer and a passive dancer. There are no unwind and rewind rollers, but there is a motor driven roller also called the master speed roller, that runs the web at speeds ranging up to 1000 fpm. There is a pneumatically loaded nip roller on the driven roller, that sandwiches the web between the master speed and itself so as to reduce slip between the web and the master speed roller. This type of an endless web platform, used exclusively for research purposes, so as to run experiments without having to use large bales of web material.

Electro-mechanical components used in this setup such as load cells, velocity and position sensors, electro-mechanical and hydraulic actuators are all coordinated by a Pentium 450-Mhz computer with a DS1103 PPC controller based on Motorola PowerPC 640e processor. For advanced I/O purposes, the board includes a slave DSP subsystem based on Texas Instruments TMS320F240 DSP micro-controller. The dSPACE software includes a GUI for managing the dSPACE boards with a source editor.

The focus of this thesis is on a passive dancer mechanism and a motorized or hydraulically-



Figure 3.1: Experimental Web Platform

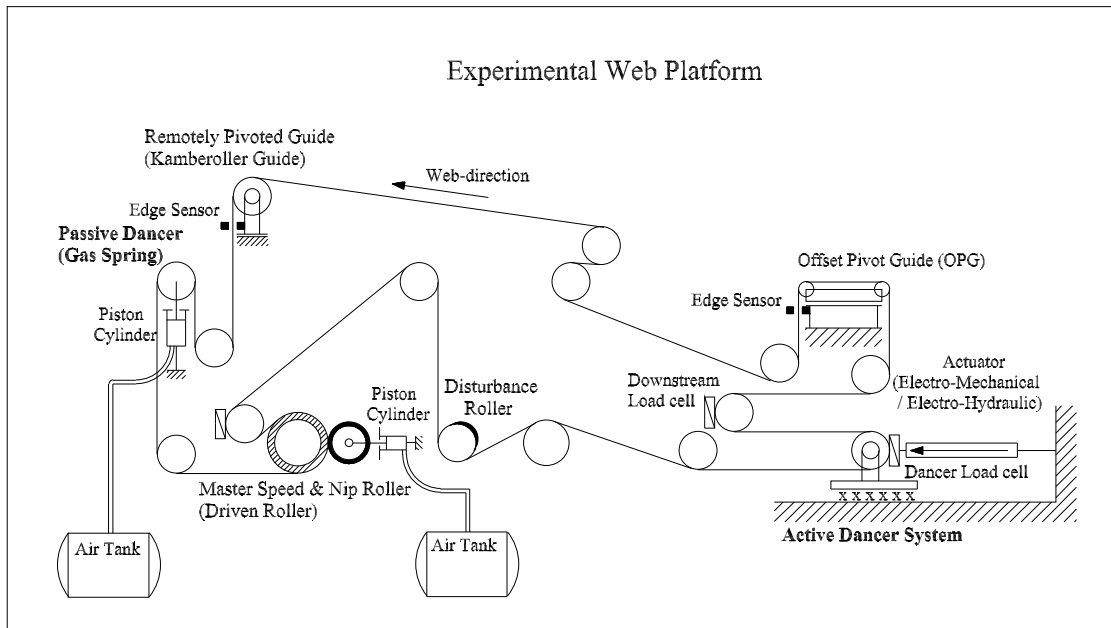


Figure 3.2: Schematic of Experimental Web Platform

cally actuated active dancer setup. There are load cells mounted on either side of the active dancer roller and these are used for tension feedback. There is an LDT (Linear Differential Transformer) used to measure the position of the dancer. This is used for position feedback. There are two other sets of load cells, one on the roller adjacent to the dancer on the downstream (downstream load cell) and the other adjacent to the driven roller on the upstream of the disturbance roller (disturbance load cell). These are used for monitoring the effects of the periodic disturbance injected into the system and its attenuation. The achievement of maximum percentage attenuation of the disturbance is the main aim of this thesis.

### 3.1 Controller Specifications

The controller is composed of a computer with a Pentium 450-Mhz computer with a DS1103 PPC controller based on a Motorola PowerPC 640e processor.



Figure 3.3: Computer

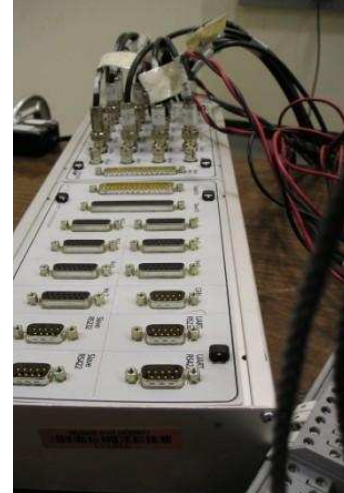


Figure 3.4: dSpace Board

### 3.1.1 The Data Acquisition Board: DS1103 board

The figures 3.3 and 3.4 show the Computer that is loaded with the data acquisition board and the connector (also a product of dSpace). The computer is equipped with the DS1103 PPC controller is a complete real-time system based on a Motorola PowerPC 640e processor. It can read from 20 channels through A/D conversion. These channels are numbered from ADCH1 to ADCH20 on the connector board. It can send output to 8 channels using D/A conversion. These are numbered from DACH1 to DACH8 on the connector board. For advanced I/O purposes, there is a slave DSP subsystem included in the board, which is based on Texas Instruments TMS320F240 DSP micro-controller.

The DS1103 PPC controller board is a standard PC/AT card that can be inserted into a PC using ISA bus as a backplane.

### 3.1.2 The dSPACE software

The base dSPACE software includes

- Control Desk software that features a GUI for managing the dSpace boards. A source editor is included and the source code is written in a C based environment.

- Microtec Power-PC C compiler Vs 1.8m is required to compile C programs. When a C program is compiled, a "FileName.ppc" file is created. This file is then used by the dSPACE board to read, interpret and send signals from the web handling system.
- The dSPACE Real-time library and the C programming interface. Using this facility, the values of parameters such as gains and reference positions or tensions can be varied online.

All the above mentioned components constitute the

### **3.1.3 Optional software packages**

The optional packages include

- A Real-time interface between Simulink and dSPACE hardware.
- Control Desk standard which offers virtual instruments.
- Multiprocessor extension.
- Test Automation.
- MLIB/MTRACE offers interface between MATLAB and dSPACE.

The packages that are regularly used are supplemented by these optional packages.

### **3.1.4 Program files for running the experiments**

In a typical experiment, the files that are included to implement a control algorithm are of four types. They are

- A C program file (FileName.c): This file consists of three main modules. A module to initialize the dSPACE board, functions for executing various tasks, which are invoked in the interrupt service routine and the interrupt routine that calls the following functions after each sampling period.

1. A/D conversion.
2. Digital I/O.
3. The Control Algorithm.
4. D/A conversion.

All the functions except the control algorithm are almost identical irrespective of the nature of the experiment. They are used solely for data acquisition purposes.

- A Layout file: This file serves as a graphical user interface to display data on the host computer. This file uses virtual instruments that can be dragged onto the control desk from a panel. Thus this file serves as a communication device between the dSPACE and the host computer.
- A trace file (FileName.trc): The parameters that are used in the control algorithm are listed in this file to be viewed in the layout file.
- The file that is created by the system on compilation of the C program. This file can be intuitively considered to be an executable application. It is automatically generated on compilation and building of the C program.

All the above files and applications form the whole set of requirements to run a successful experiment on any electro-mechanical system.

### **3.2 Web guiding systems**

There are two kinds of mechanisms available for the guiding of the web on the machine. Guiding is very important because due to variations in web velocities and tension, the web has a tendency to deviate from its path in the lateral direction (towards its sides) and slip out of the rollers. This causes undesirable problems in further processing of the web.



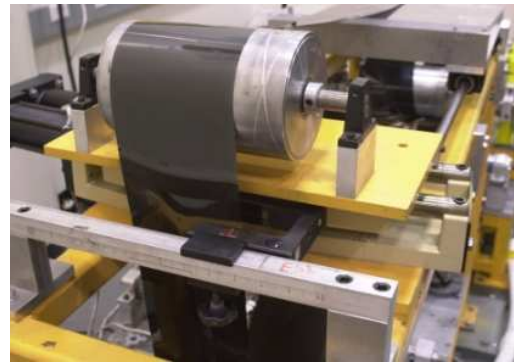
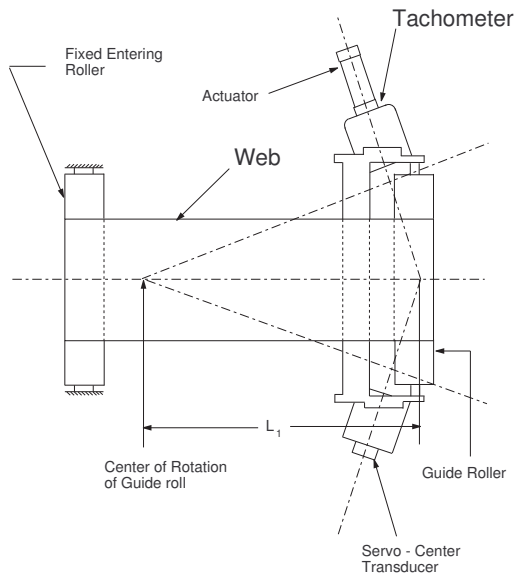


Figure 3.5: Remotely Pivoted Guide and Edge Sensor

The guides are controlled using a PI controller and the feedback is obtained using the edge sensors that are located immediately on the downstream side of the respective guides. These edge sensors operate on ultrasonic sensing.

The two guides are found on either ends of the machine and effectively control the lateral movement of the web thereby keeping it within limits.

### 3.2.1 Remotely Pivoted Guide (Kamberoller)

The figures 3.2.1 and 3.2.1 show the FIFE Kamberoller with its edge sensor and its schematic representation. The kamberoller guide is positioned right before the passive dancer between a couple of idler rollers. It is an assembly of a roller, a roller carriage, a couple of guide rails on which the guide moves and an electro-mechanical actuator fitted with a motor. There is an edge sensor that is fitted on the guide assembly itself. It is an infrared sensor and used for feedback, by the A9 controller of the kamberoller. The details of the A9 controller is discussed later under a separate heading.

The kamberoller guide is called a remotely pivoted guide (RPG) because the guide moves along a circular path and the center of the guide is far outside the guide assem-

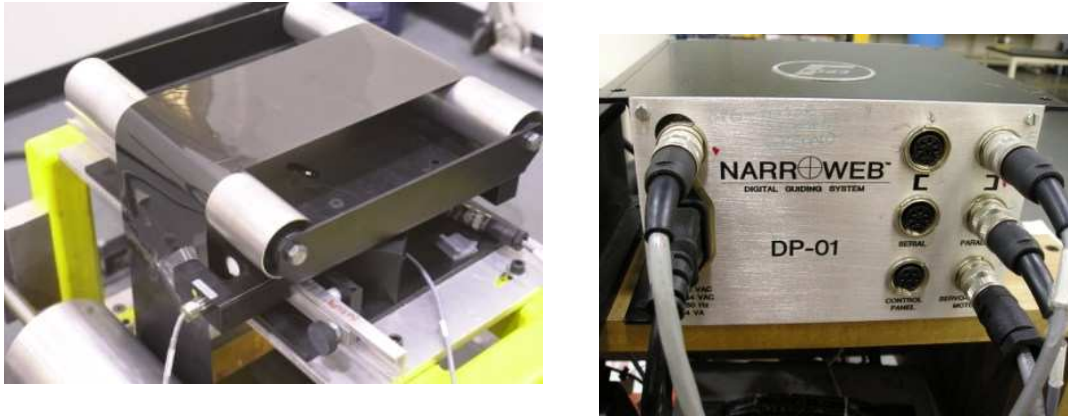


Figure 3.6: Offset Pivot Guide, edge sensor and Narrowweb DP-01 controller

bly. The radius of curvature of the guide path is much greater than the size of the guide itself. The roller has an electro-mechanical actuator where the rotation of the motor is converted to linear displacement in the lateral direction. The actuator motor has an in-built tachogenerator that measures its rotational speed. The kamberoller mechanism is run by its A9 directly. It may be bypassed and run using a computer. Hence for all practical purposes in this thesis the A9 is used for control of the kamberoller guide.

### 3.2.2 Offset Pivot Guide (OPG)

The figures 3.2.2 and 3.2.2 show the offset pivot guide and the narrowweb DP-01 controller. The OPG guide is positioned at the downstream side of the active dancer between two idler rollers. It is an assembly with two rollers (having smaller diameters), positioned parallel to each other on a carriage. The whole carriage rotates about a pivoted point. The OPG guide unlike the kamberoller, has a pivot within its assembly (that is actually beneath one of the rollers), but is a little offset from its geometric center .

It has a little proximity sensor built into it so as to enable it to position itself in the center with respect to the web line. The 'OPG center' is the position at which the rollers of the OPG are aligned with their axes perpendicular to the web direction.

### 3.2.3 The RPG Guide Controller (The A9 Processor)



Figure 3.7: The A9 Controller

The figure 3.7 shows the A9 processor that is used for the FIFE Kamberoller guide. The A9 processor is a versatile analog controller that can be used to control many closed loop subsystems individually if their contribution to the overall experiment is negligible. The significance of the guides discussed above is only for lateral position control of the web (mainly to avoid the slippage of web out of the rollers). Hence web guiding and lateral control can be taken care of by the A9 processor.

There are three modes at which the A9 can be operated, viz. manual, auto and servo center.

### 3.3 Load cells

The load cells are used in pairs for measuring web tension at three different places along the closed web loop.

- One pair on the active dancer roller (Dancer Load cells).
- One pair on the roller immediately on the downstream of the active dancer roller (Downstream Load cells).
- One pair on the roller immediately on the upstream of the passive dancer roller (Disturbance Load cells).

### **3.3.1 Dancer Load cells**

These are cantilever load cells from MAGPOWR. Their model number is CL2-50 and are specifically designed for narrow web applications, accommodating cantilevered idler rollers in processing machines which have only one side frame.

The load cells are ruggedly constructed for long life and dependability with built-in mechanical overload stops. A full wheatstone bridge strain gauge arrangement is incorporated in each load cell to provide accurate means of measuring tension. They are designed to measure tensions up to 50lbs in either direction.

### **3.3.2 Downstream Load cells**

The figure 3.8 shows the pair of downstream load cells that are used to monitor the disturbances that the active dancer attempts to attenuate. These are rugged load cells, used in pairs for web applications and are capable of measuring loads up to 50 lbs. The position of these load cells help monitor the attenuation of tension disturbances while the active dancer is used.

### **3.3.3 Disturbance Load cells**

The figure 3.9 shows the picture of the disturbance load cell pair. The disturbance load cells are positioned on the downstream of the passive dancer just before the master speed roller. These can be employed to monitor the disturbances injected into the system from a remote



Figure 3.8: The downstream load cell

location. These are generally used for measuring the attenuation of tension disturbances while conducting experiments on the passive dancer.

### 3.4 Master Speed Roller

The left picture in figure 3.4 shows the master speed roller, the nip roller loaded using the pneumatic system and a portion of the gearbox used for speed reduction. The picture on the right shows the control panel with knobs for adjusting the speed of the master speed and the pressure for the nip roller and the passive dancer. The Motor Driven roller is called the master speed roller. This roller is directly connected to the motor using a belt drive for speed reduction. The diameter of the roller is 8 inches and its width is 8 inches as well.

It is also fitted with a tachometer to measure the speed of the motor. There is an analog controller for the speed control of the motor.



Figure 3.9: Disturbance load cell

### 3.4.1 Nip Roller

There is a nip roller that is operated pneumatically and is designed to constantly remain in contact with the master speed roller. The nip roller is 5 inches in diameter and 8 inches in width. Its surface is made of soft rubber-like material, so as to increase the area of contact on the master speed roller. This increases the friction between the web and the master speed thereby reducing slip.

The nip rollers are pressed against the master speed roller with the aid of a piston and cylinder mechanism into which air is forced at a set pressure. This pressure could be raised or lowered using the knobs on the master speed control panel. The air supply is buffered in the red cylinders as shown so as to reduce the pressure fluctuations. The gas tanks shown

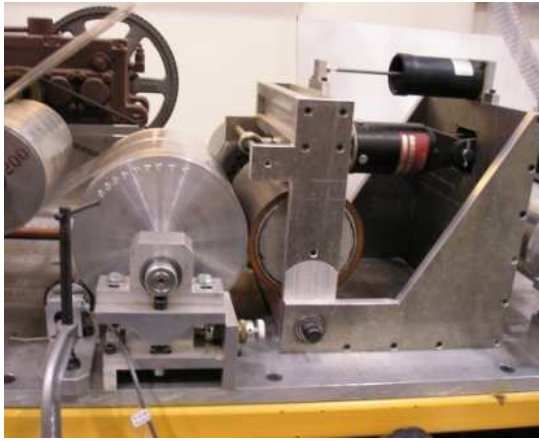


Figure 3.10: Master speed roller, nip roller, tacho-generator and its control panel



Figure 3.11: Gas tanks for nip roller and passive dancer

in the figure 3.11 are used one each for the nip roller and the passive dancer.

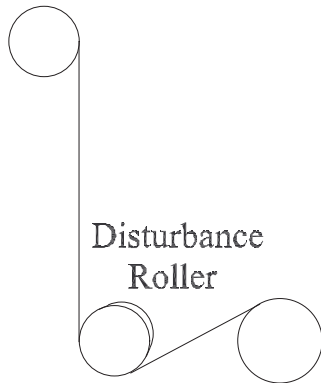


Figure 3.12: Schematic and Picture of Disturbance roller

### 3.5 The Idler Rollers

The idler rollers are identical, all of the equal diameter (approx. 5.0 in) and width (8.0 in). They are made of aluminum and are mounted on their respective shafts using ball bearings. The shafts are fixed and held on the main frame of the machine.

The rollers are grooved in one way or the other that are shown in the two figures. These grooves are meant to avoid variations in tensions due to air inclusions. The rollers are not cambered and are assumed to have negligible bearing friction for control purposes.

### 3.6 Disturbance Injection in the web line

The figures 3.6 and 3.6 show the disturbance roller and its schematic representations respectively. The arrangement for injecting the disturbance into the system while running experiments with the active dancer is an idler roller. It is loaded with a strip of rubber that gives an eccentricity to the web thereby causing a periodic variation in web tension. This is a way to inject the periodic disturbance into the web line. The active dancer roller is just a couple of rollers away from the disturbance roller on its downstream side (so as to be most affected by the disturbance). The strip is secured on the roller using a couple of screws on



either side.

The web drives the disturbance roller on account of the friction between them. At higher web tensions (10lbs or greater) there is negligible slip between the roller and the web. So the period of disturbance can be varied by varying the web velocity. The magnitude of the disturbance can be varied by varying the thickness of the rubber strip.

For the passive dancer experimental setup there are two options available for injecting a disturbance. One is using the above mentioned rubber-strip setup, and the other using the active dancer itself. The actuator that is mounted on the active dancer is can be used to move the dancer back and forth in various patterns so as to vary the tensions. One advantage of this mechanism is that the period of variation of tension does not have to be dependent on the web velocity, as the web does not drive the disturbance.

### **3.7 Dancers Rollers**

The dancer rollers are primarily idler rollers that are mounted on carriages having one degree of freedom i.e. they are free to move either in translational direction (mounted on slides) or in rotational direction (hinged on a frame). The type of dancer system is chosen based on the application requirements, space constraints and other such factors. The types of dancers that are dealt with in this thesis, are translational. They slide on cylindrical rails.

There is further division on the basis of whether the carriage is loaded with an actuator. The presence of an actuator for dancer action makes it an active dancer and otherwise a passive dancer.

#### **3.7.1 The Passive Dancer**

The figures 3.14 and 3.13 show the passive dancer and its schematic representations respectively. The passive dancer system that is set up in the machine is composed of two elements viz., mass of the carriage added to that of the roller and a dashpot into which compressed air is forced. The compressibility of air and the elasticity of the web may be thought of

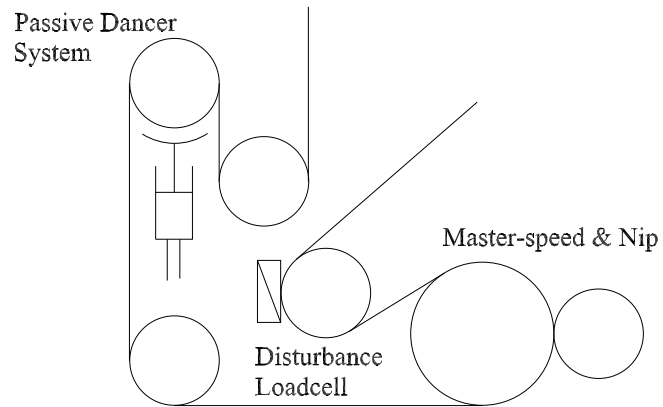


Figure 3.13: Schematic of Passive Dancer mechanism



Figure 3.14: The passive dancer

as a virtual gas spring. A mass-spring-damper system is formed, which with the aid of its inherent dynamics, attempts to attenuate the variation in tension.

The passive dancer carriage is mounted on vertical guides and slides up and down with the gas spring arrangement forcing the dancer in the upward direction. The weight of the carriage adds to the web tension while opposing the gas pressure. In this thesis the gas pressure is varied from 12 psi to 20 psi in steps of 2 psi depending on the web tension and disturbance. There is a buffer cylinder to maintain the pressure within acceptable tolerances of fluctuations. The angle of wrap of the web around its roller is about 180 degrees. This is the recommended wrap to simplify the mathematical modeling and aid in calculations. The buffer cylinders are shown in figure 3.11.

The passive dancer is found to be successful in attenuating periodic disturbances with low frequencies. Its response is limited to the low frequency disturbances and at frequencies equal to or higher than its natural frequencies, it is a failure. Hence it is said to have a small bandwidth.

The passive dancer is also constantly subjected to tension variations caused by the Remotely pivoted guide when the web moves in the lateral direction. This disturbance is significant at times and sometimes causes major oscillations.

### **3.7.2 The Active Dancer**

The figures 3.16 and 3.15 show the active dancer and its schematic representations respectively. An active dancer can be utilized for periodic disturbances that have a high frequency of occurrence (in the order of 2 Hz and above). The periodic disturbance that is considered in this thesis is injected into the system in the form of roller eccentricity and hence is directly proportional to the roller velocity which in turn is proportional to the web velocity.

The active dancer though slides back and forth in the horizontally arranged rails. These rails have very less friction at their contact points with the bearings. The active dancer carriage has a metal rod attached to it, which used to center it with respect to the total

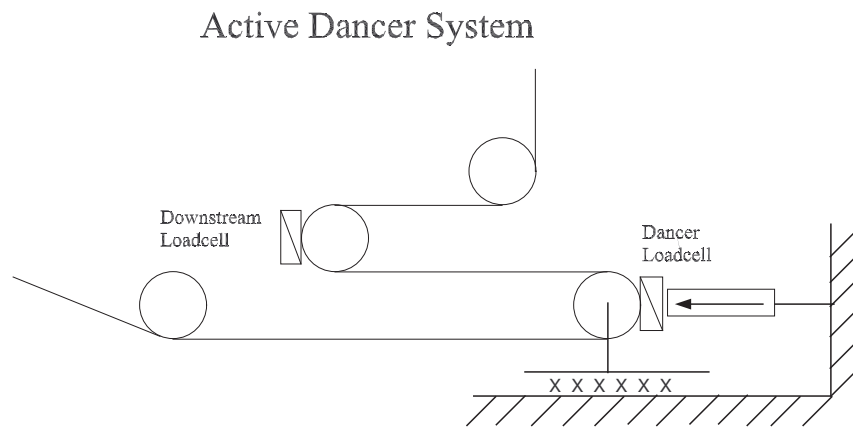


Figure 3.15: Schematic of Active Dancer



Figure 3.16: Active Dancer with Load cell and Position Sensor

length of travel using a proximity sensor. This is very useful in cases where there is no position sensor (LDT)

### **3.8 Actuators for Active Dancer**

The two types of actuators that the active dancer is driven with. An electromechanical actuator and a hydraulic actuator.

#### **3.8.1 Electro-mechanical Actuator**

The electromechanical actuator has a motor and a belt drive followed by a screwed drive all in series to achieve the final translational motion, which is given to the carriage of the dancer.

There is a tachometer integrated with the motor assembly. This is used as a feedback by the CSP-01 controller that the active dancer is connected to. This may also be used for velocity feedback by the computer if the controller is bypassed.

There is also a proximity sensor attached to the dancer assembly that with the aid of a steel rod attached to the dancer carriage, can be used to center the dancer with respect to the total guide length.

#### **3.8.2 The Electro-Hydraulic Actuator**

The figure 3.17 shows the hydraulic actuator. The hydraulic setup is a FIFE Corporation product. It has an oil tank, a servo valve and a piston cylinder arrangement. The piston is attached to the dancer carriage.

A three phase motor keeps the pressure of the oil in the system at approximately 500 psi. There is a pressure gauge that measures this pressure and also displays the change in pressure when the piston is in motion. The oil that is used for its operation is a fluid of quality AW-32 with a viscosity of 60 to 450 SUS at 100 degree Fahrenheit ( in this case it is Valvoline W760).

The servo-valve and its schematic are shown in the figures 3.8.2 and 3.8.2 respectively. The actuator signal from the computer is given to the servo valve, through a signal ampli-

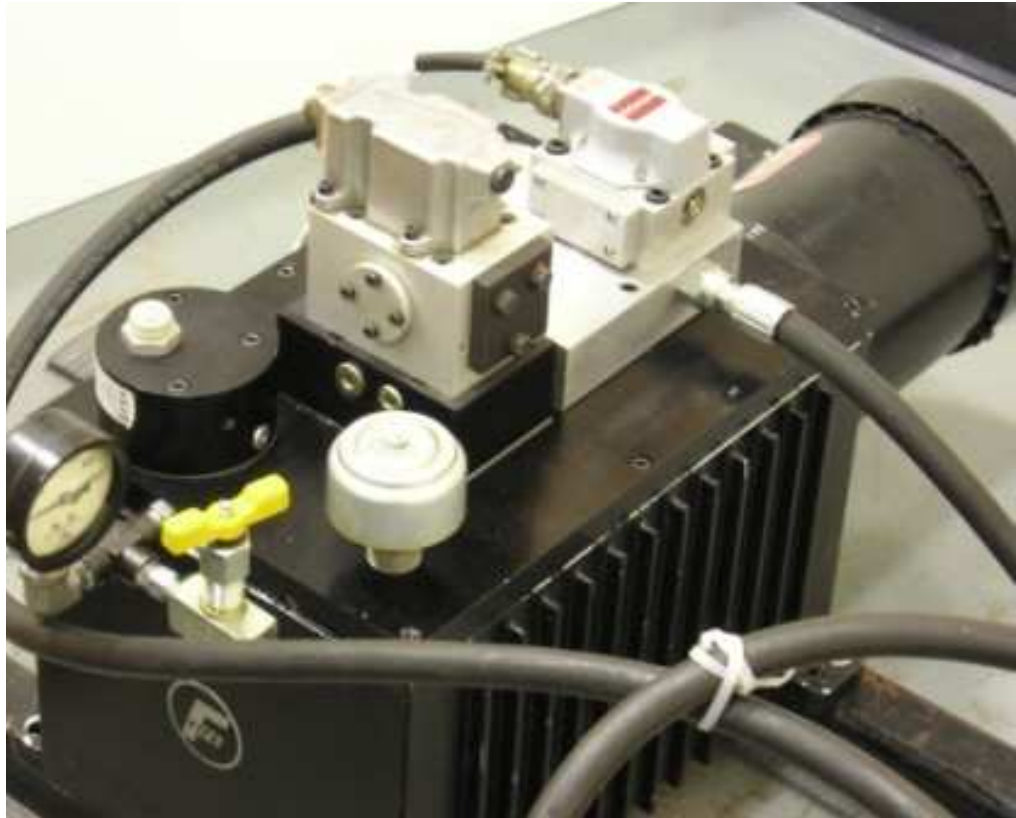


Figure 3.17: The hydraulic actuator

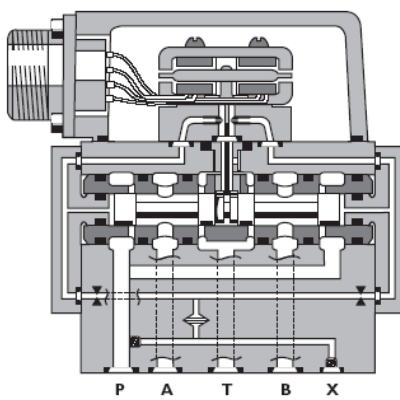


Figure 3.18: The Moog servo-valve



Figure 3.19: The CSP-01 controller

fier, which opens and closes appropriately to operate the piston-cylinder mechanism. The schematic and picture of the servo-valve is shown in the figure. The piston cylinder mechanism is a product of Parker cylinders that is as shown in the figure. It is mounted on the active dancer frame and the piston rod is connected to the carriage.

This valve has a dead zone where equal pressure is given on both sides of the piston in the cylinder. This results in a dead-lock when zero voltage is given to the servo-valve. The amplifier is custom made by FIFE corporation called "FIFE logic control driver". Its part number is 84666 – 01 *c – i – 1 – 0*. A custom made power supply gives DC power to the amplifier.

There is provision on the piston cylinder arrangement for the LDT that is described in the earlier section.

### 3.8.3 The CSP-01 Controller

The figure 3.19 shows the CSP-01 controller. The CSP-01 controller, also a product of FIFE, is similar to the A9 controller discussed with respect to the RPG guide. This controller is used for analog control of the tension based on velocity feedback of the electromechanical actuator. It operates in three modes as follows,

- Manual mode where the two push buttons located at the top can be used for moving the dancer back and forth for manual adjustment of the tension.
- Auto mode where the analog controller of the CSP itself can be put into action. The gain can be adjusted using the knob located on the right side.
- Servo center mode where the control can be obtained through the line in from a computer. This is the mode most frequently used for control in this thesis.

It has an in built DC power supply and plugs directly into the AC main supply.

## 3.9 Web Materials

The figure 3.20 shows the two web materials that were used for running experiments on the machine. One is an opaque black colored stiff plastic web of very high young's modulus and high strength. The other web is a white paper which is more viscoelastic compared to the opaque web.

The specifications of the web materials that have been used for running experiments are as listed below.

For the black polythene web,

$$E = 871,459 \text{ lbf/in.}^2 \quad (3.1)$$

$$EA = 14,117 \text{ lbf} \quad (3.2)$$

$$\text{Thickness} = 0.003 \text{ in.} \quad (3.3)$$

$$\text{Web width} = 5.40 \text{ in.} \quad (3.4)$$





Figure 3.20: The webs used for experiments

For the white paper web,

$$E = 102660 \text{ lbf/in.}^2 \quad (3.5)$$

$$EA = 2090 \text{ lbf} \quad (3.6)$$

$$\text{Thickness} = 0.006 \text{ in.} \quad (3.7)$$

$$\text{Web width} = 6 \text{ in.} \quad (3.8)$$

## CHAPTER 4

### EXPERIMENTAL RESULTS AND CONCLUSIONS

The experiments that were run on the traction machine for the purpose of this thesis, fall under the two broad categories.

1. Attenuation of sinusoidal tension disturbances using passive dancer, loaded on an air spring.
2. Attenuation of sinusoidal tension disturbances using the active dancer, with a motorized or hydraulic actuator.

#### 4.1 Experiments using passive dancer setup

The experiments that were run on the passive dancer setup were run using two webs of distinct characteristics. The specifications of the webs are listed in chapter 3.

The figures show the attenuation of a periodic disturbance that is sinusoidal. The disturbance is injected using the active dancer actuator. The sinusoidal disturbance in this case is approximately  $10 \sin \omega t$  lbs.

In the plots, the first 20 seconds of the plot shows the disturbance experienced at the load cells when the passive dancer is arrested at its mean position. The next 20 seconds show the disturbance attenuation phase. The difference in the tension variation in these two phases is the magnitude of rejection attained.

It is observed that the first half of both the set of plots are different despite the fact that identical disturbance is injected. This is because of the difference in the Modulus of elasticity (Young's modulus) of the web materials. The black web is stiffer with a high

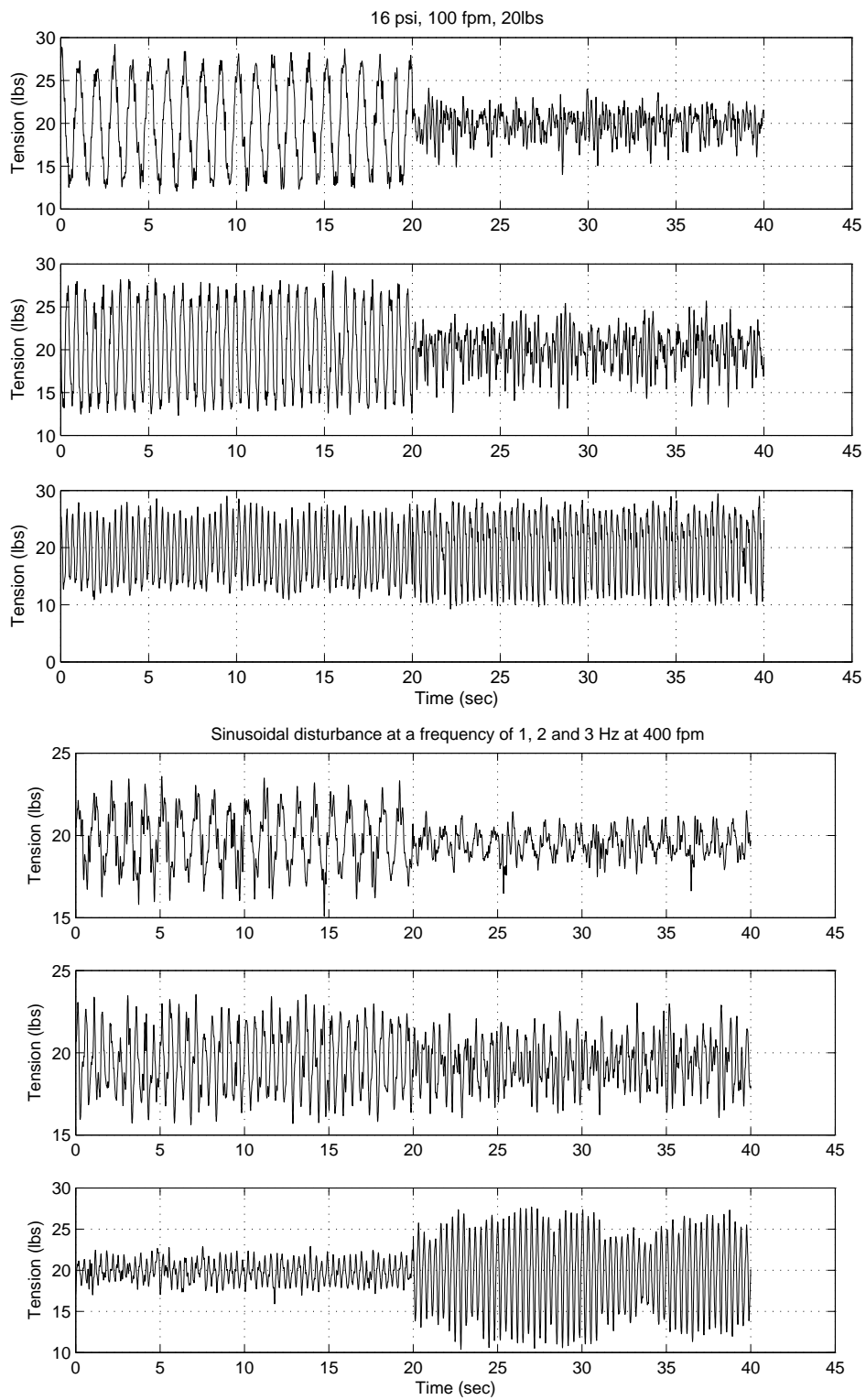


Figure 4.1: Plots showing attenuation using passive dancer at 16 psi and 12 psi respectively

Young's modulus and hence transmits more of the actual disturbance to the load cell and the passive dancer than the white web.

The disturbance frequency is varied from 1 hz. to 3 hz. The passive dancer performance deteriorates with the rise in disturbance frequency. This trend in the behavior is predicted using the dynamic equations of the passive dancer mechanism. Every passive dancer is associated with an inherent natural frequency. When this frequency is approached it oscillates with a large amplitude, thereby delivering a high gain in magnitude. This is the reason it ceases to attenuate.

## **4.2 Experiments using active dancer setup**

The figures 4.2 and 4.2 show the various frequencies of disturbances for the first 15 seconds and the attenuation by the active dancer operated using a hydraulic actuator.

The black web material is chosen for running this experiment because it propagates most of the disturbance through it to the dancer. This is due to the high stiffness it possesses. At high frequencies though, the magnitude of disturbance seems to reduce.

The controller that is used to attenuate the disturbances is the internal model controller(IMC) controller. This seems to be the most effective of the controllers in this case primarily because the periodic disturbance here is sinusoidal in nature. There is an internal disturbance model in the IMC controller that compensates for the disturbance.

At high frequencies the PID controller does not function satisfactorily. The desired attenuation is not achieved; in fact the disturbance gets amplified which is highly undesirable.

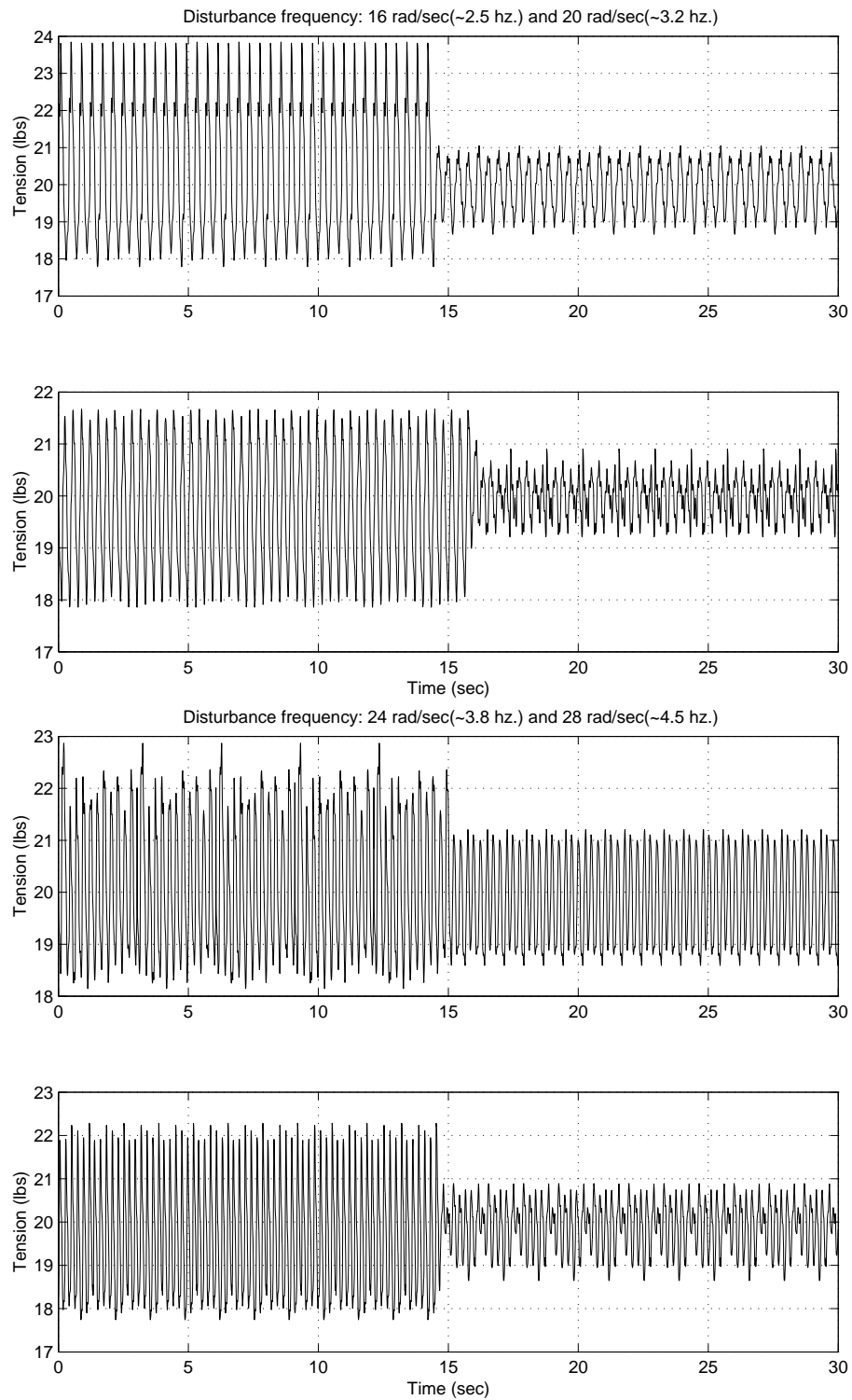


Figure 4.2: Plots showing attenuation using active dancer with hydraulic actuator

<i>Disturbance</i>	<i>% Attenuation in Amplitude</i>		
<i>Frequency</i>	<i>Passive Dancer</i>		<i>Active Dancer</i>
<i>(Hz.)</i>	<i>Polythene Web</i>	<i>“Tyvec” Paper</i>	
1	75	50	-
2	45	20	-
2.5	-	-	60
3.2	-	-	50
3.8	-	-	50
4.5	-	-	50

Table 4.1: Percentage attenuation in the periodic disturbance

### 4.3 Conclusions

The conclusions can be enumerated as follows.

1. The passive dancer observed seen to be performing better at lower frequencies viz. up to 2 Hz. At higher frequencies either there is no response or there is amplification.
2. The active dancer with the hydraulic actuator is observed to be performing better than the passive dancer at periodic disturbances of high frequencies, especially with the IMC controller.

## CHAPTER 5

### SUMMARY AND FUTURE WORK

#### 5.1 Summary

This thesis can be summarized as follows.

- A model for the active dancer is developed using the web dynamic equations.
- A model for the passive dancer is developed using the web dynamics and the concept of gas-springs.
- A detailed description of the Experimental web platform is presented with all the transducer calibrations.
- The hydraulic actuator for the active dancer was setup, experiments were run with sinusoidal disturbances and attenuation achieved up to a frequency of  $28rad/sec$ .
- An experimental evaluation of the attenuation achieved by passive and active dancer is performed.
- A comparative study of the two types of dancers is carried out.
- A comparative study of two types of web material is carried out.

## 5.2 Future Work

The future work that can be pursued with this direction of approach is enumerated as follows,

1. The passive and active dancer approach for attenuating periodic disturbances can be tried with web materials of various Young's modulus.
2. A hydraulic actuator with better performance viz. with faster response can be installed and used.
3. A dual actuator can be used. The hydraulic actuator can be coupled with a piezoelectric actuator where the disturbances are of high frequencies.
4. Other monatomic gases can be investigated for better performance compared to the air spring viz. helium.



## BIBLIOGRAPHY

- [1] D.P. Campbell, *Dynamic Behavior of the Production Process, Process Dynamics* (John Wiley and Sons, Inc., New York, First edition, 1958).
- [2] K.P. Grenfell, Tension control on paper-making and converting machinery, in: *Proceedings Ninth IEEE Annual Conference on Electrical Engineering in the Pulp and Paper Industry* (Boston, MA, June, 1963) 20–21.
- [3] D. King, The mathematical model of a newspaper press, *Newspaper Techniques* (December, 1969) 3–7.
- [4] G. Brandenburg, New mathematical models for web tension and register error, in: *Proceedings International IFAC Conference on Instrumentation and Automation in the Paper, Rubber, and Plastics Industry 1* (1977) 411–438.
- [5] G.E. Young and K.N. Reid, Lateral and longitudinal dynamic behavior and control of moving webs, *ASME Journal of Dynamic Systems, Measurement, and Control* **115**, (1993) 309–317.
- [6] W. Wolfermann, Tension control of webs, a review of the problems and solutions in the present and future, in: *Proceedings Third International Conference on Web Handling* (Stillwater, OK, June, 1995) 198–229.
- [7] D. H. Carlson, Considerations in the selection of a dancer or load cell based tension regulating strategy, in: J.K. Good, ed., *Proceedings Sixth International Conference on Web Handling* (Stillwater, OK, 2001), 243–262.

- [8] N. A. Ebler, R. Arnason, G. Michaelis, and N. D. Sa, Tension control: Dancer rolls or load cells, *IEEE Transactions on Industry Applications* **29** (1993) 727–739.
- [9] J. J. Shelton, Limitations to sensing web tension by means of roller reaction forces, in: J.K. Good, ed., *Proceedings Fifth International Conference on Web Handling*, (Stillwater, OK, 1999).
- [10] K. Reid and K. Lin, Dynamic behavior of dancer subsystems in web transport systems, in: J.K. Good, ed., *Proceedings Second International Conference on web handling*, (Stillwater, OK, 1993) 135–146.
- [11] G. Rajala, Active dancer control for web handling machine, *Master's thesis*, University of Wisconsin-Madison, August 1995.
- [12] G. Rajala, Controlling web tension by actively controlling velocity of dancer roll, tech. rep., United States Patent Number 5,602,747, February 1997.
- [13] P. R. Pagilla, R. V. Dwivedula, Y.-L. Zhu, and L. P. Perera, The role of active dancers in tension control of webs, in: J.K. Good, ed., *Proceedings Sixth International Conference on Web Handling*, (Stillwater, OK, 2001), 227–242.
- [14] P. R. Pagilla, R. V. Dwivedula, Y. Zhu, and L. P. Perera, Periodic tension disturbance attenuation in web process lines using active dancers, *ASME Journal of Dynamic Systems, Measurement, and Control* **125** (2003) 361–371.
- [15] P. R. Pagilla, R. V. Dwivedula, and Y.-L. Zhu, The role of active dancers in tension control of webs, tech. rep., Oklahoma State University, Stillwater, October 2002. WHRC Project 9798-1.
- [16] K. Shin, K. Reid, and S. Kwon, Non-interacting tension control in a multi-span web transport system, in: J.K. Good, ed., *Proceedings Third International Conference on Web Handling* (Stillwater, OK, 1995) 312–326.

- [17] P. Lin and M. Lan, Effects of PID gains for controller design with dancer mechanism on web tension, in: J.K. Good, ed., *Proceedings Second International Conference on Web Handling* (Stillwater, OK, 1993) 66–76.
- [18] K. Shin, Distributed Control of Tension in Multi-Span Web Transport Systems. PhD thesis, Oklahoma State University, Stillwater, May 1991.
- [19] B. C. McDow and C. D. Rahn, Adaptive web-tension control using a dancer arm, *Tappi Journal* **81** (1998) 197–205.
- [20] L. P. Perera, The role of active dancers in tension control of webs, Master's thesis, Oklahoma State University, Stillwater, 2001.
- [21] S. Skogestad and I. Postlethwaite, *Multivariable Feedback Control: Analysis and Design* (John Wiley & Sons, 1996).
- [22] K.J. Astrom and B. Wittenmark, *Adaptive Control* (Addison-Wesley Publishing Company, Inc., Reading, Massachusetts, 1995)
- [23] G. Brandenburg, The dynamics of elastic webs threading a system of rollers, *Newspaper Techniques* (1972) 12–25.
- [24] D.P.D. Whitworth and M.C. Harrison, Tension Variations in Pliable Material in Production Machinery, *Journal of Applied Mathematical Modeling* **7** (1983) 189–196.
- [25] J.J. Shelton, Dynamics of web tension control with velocity or torque control, in: *Proceedings of the American Control Conference* (Seattle, 1986) 1423–1427.
- [26] M. Morari and E. Zafiriou, *Robust Process Control* (Prentice Hall, Englewood Cliffs, 1989).

## APPENDIX A

### Experiments on Black polythene web

This appendix contains all the experimental results that were run. The following results are for the black opaque web.

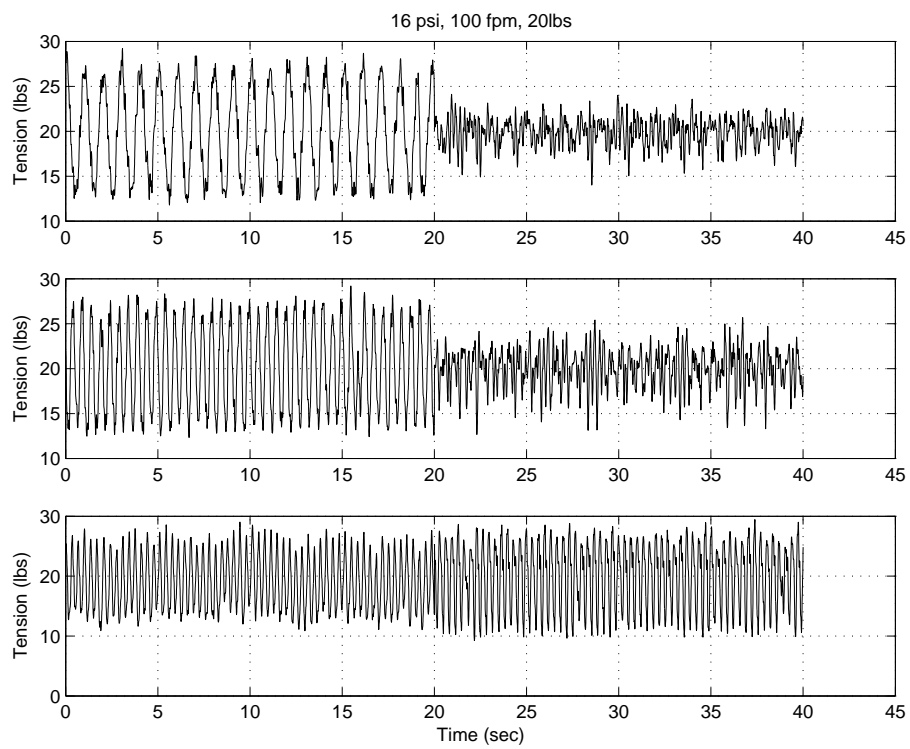


Figure A.1: Plots with disturbance attenuation at 100 fpm at 16psi

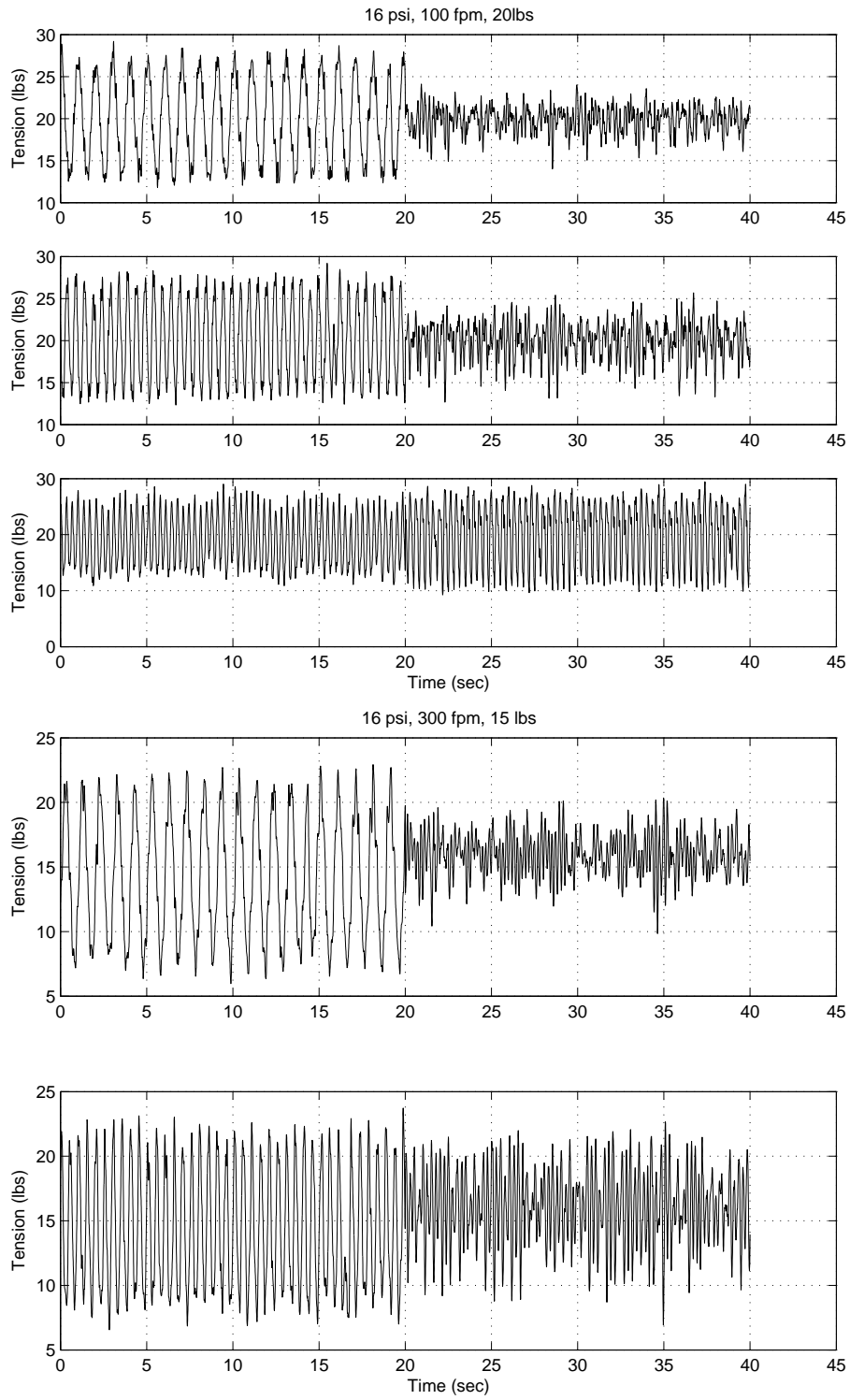


Figure A.2: Plots with disturbance attenuation at 200 and 300 fpm at 16psi

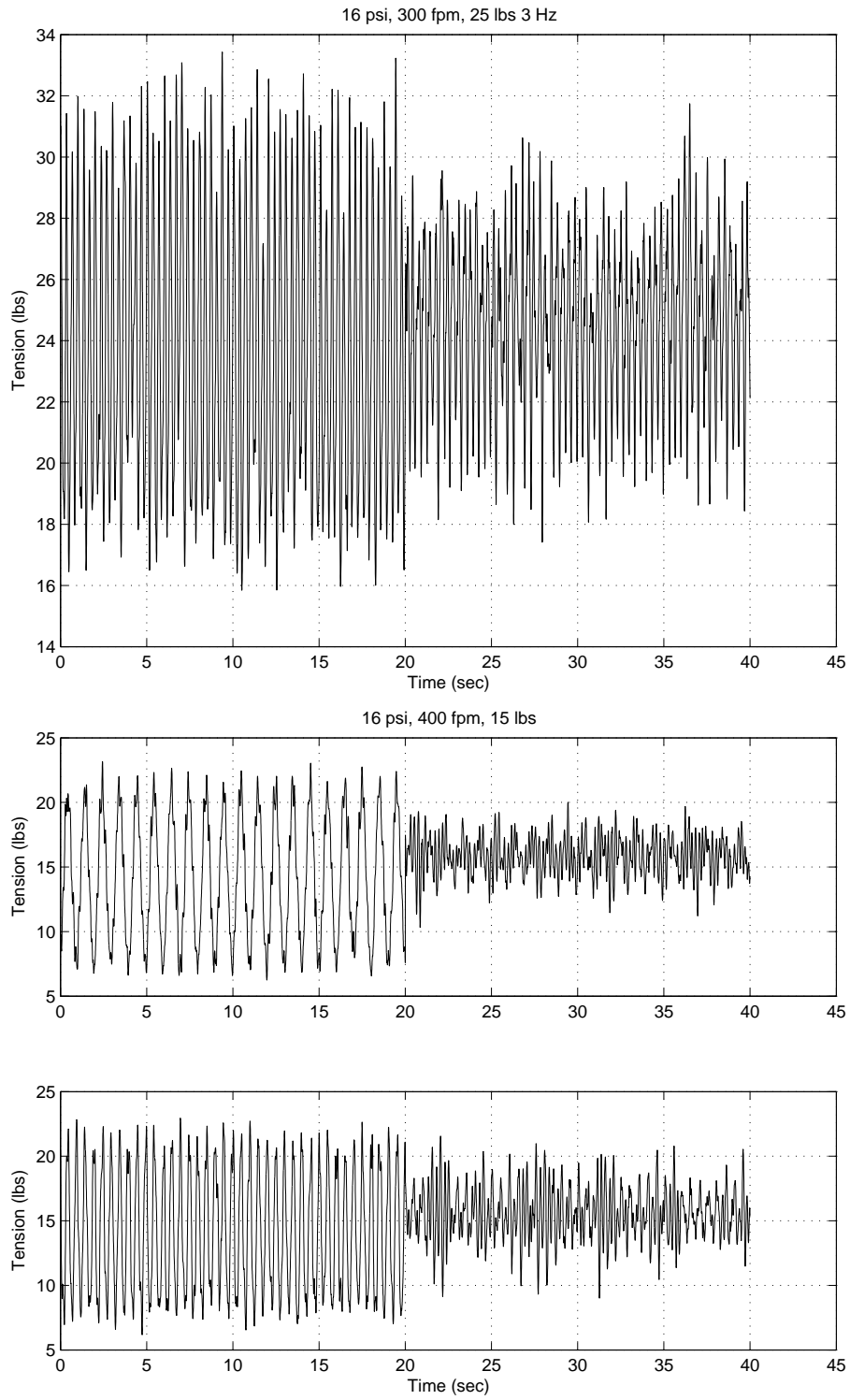


Figure A.3: Plots with disturbance attenuation at 300 and 400 fpm at 16psi

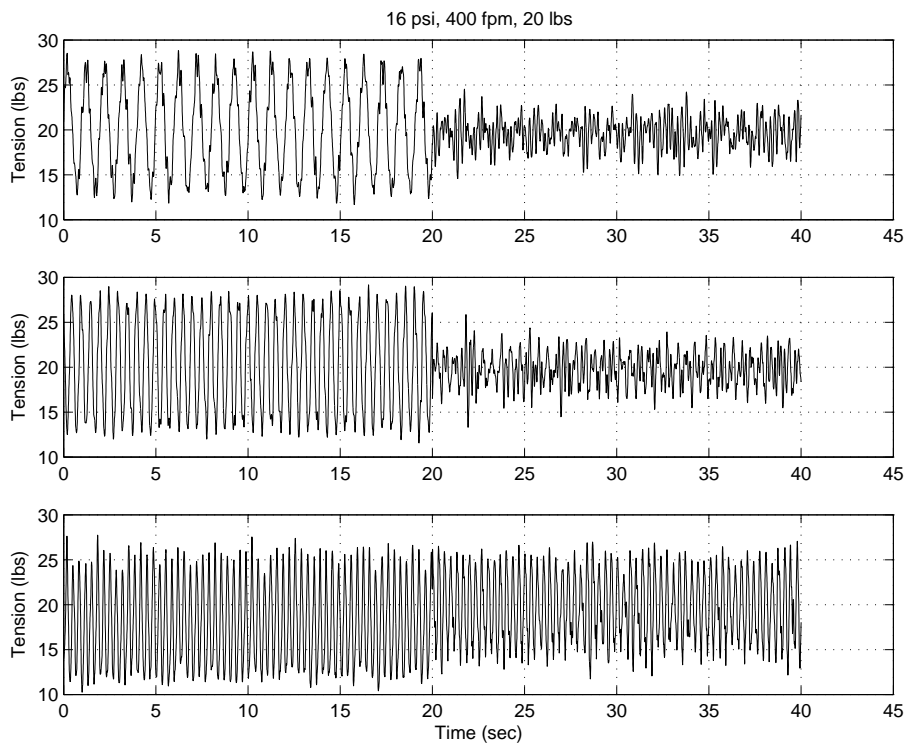


Figure A.4: Plots with disturbance attenuation at 400 fpm at 16psi

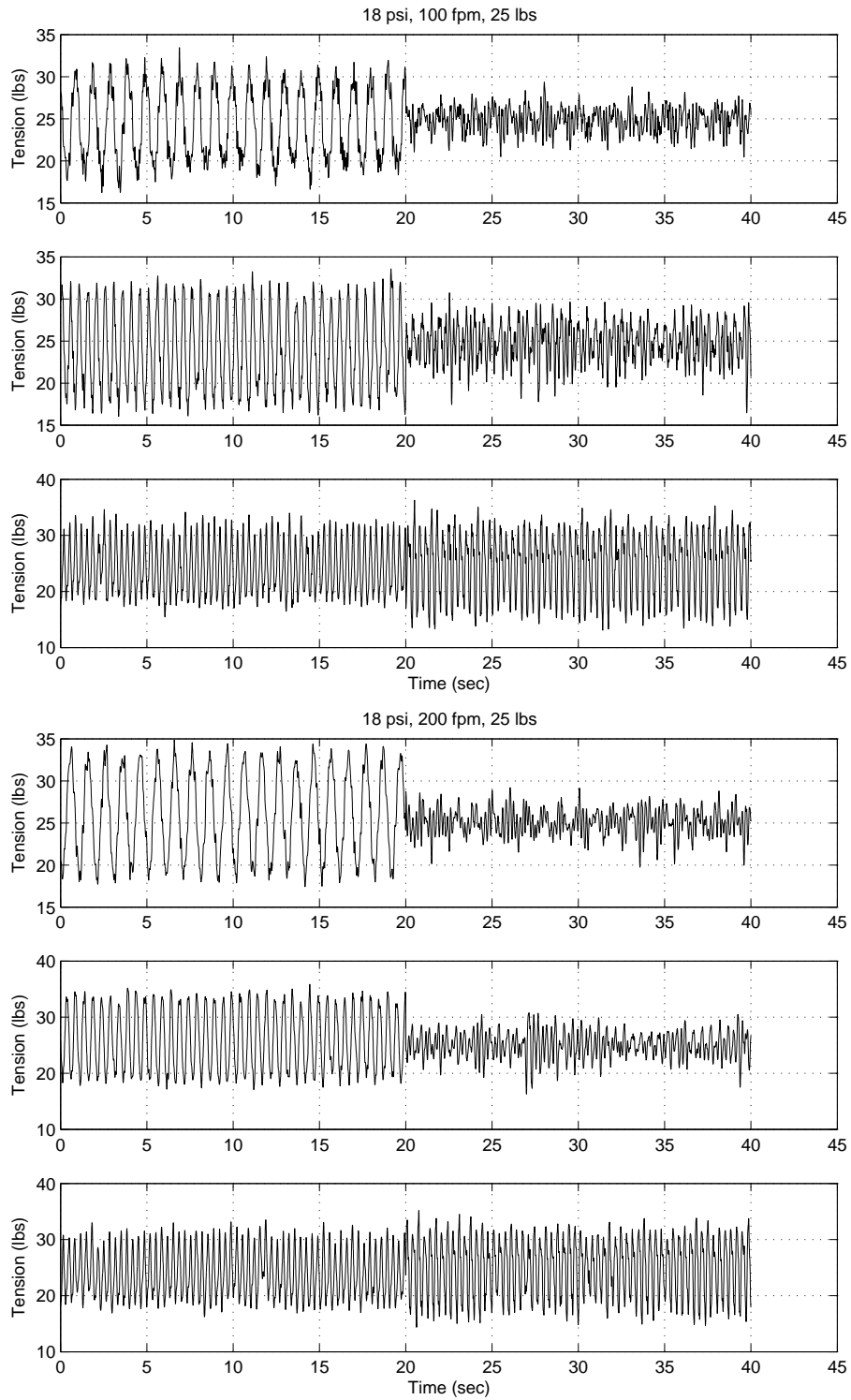


Figure A.5: Plots with disturbance attenuation at 100 and 200 fpm at 18psi



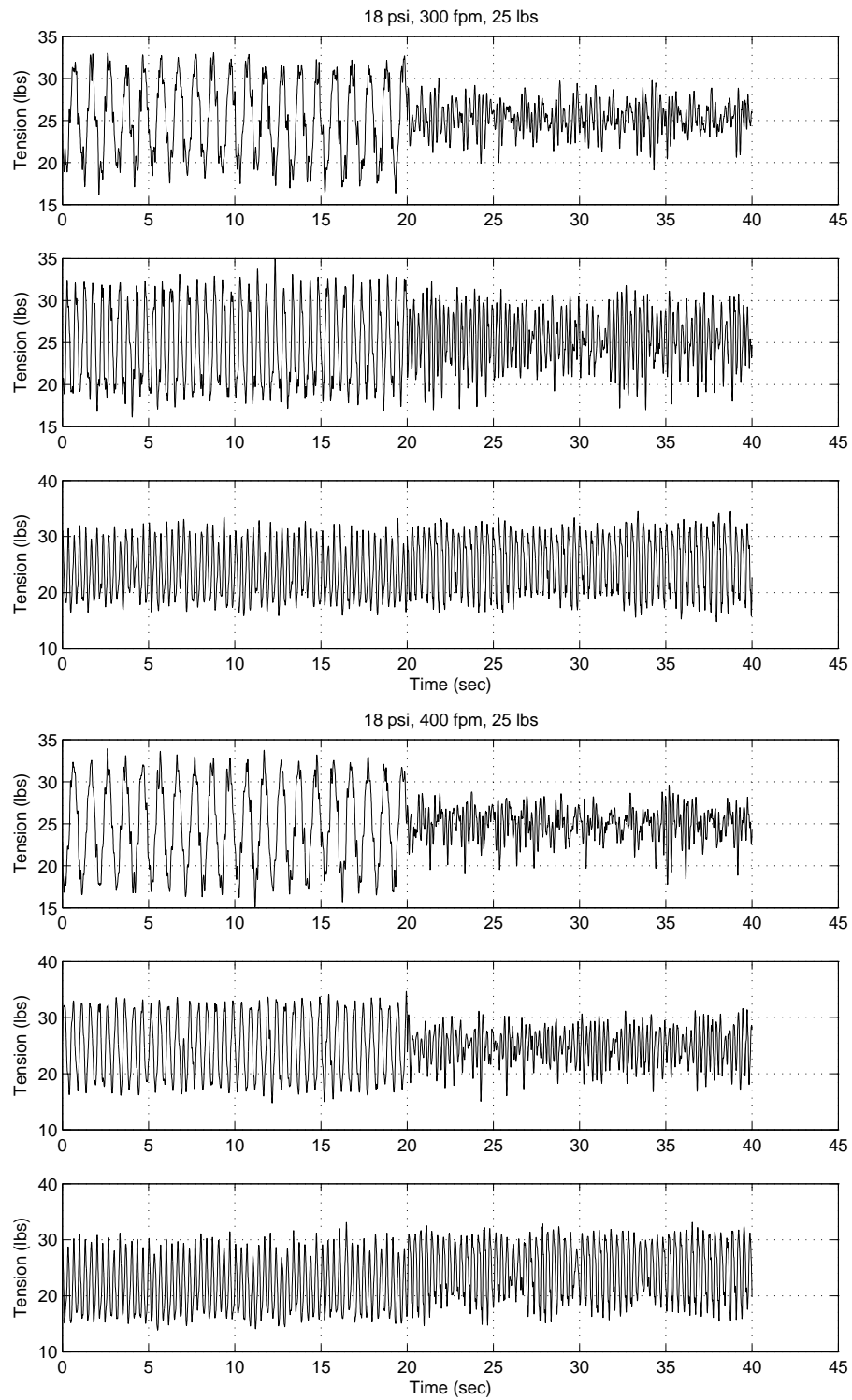


Figure A.6: Plots with disturbance attenuation at 300 and 400 fpm at 18psi

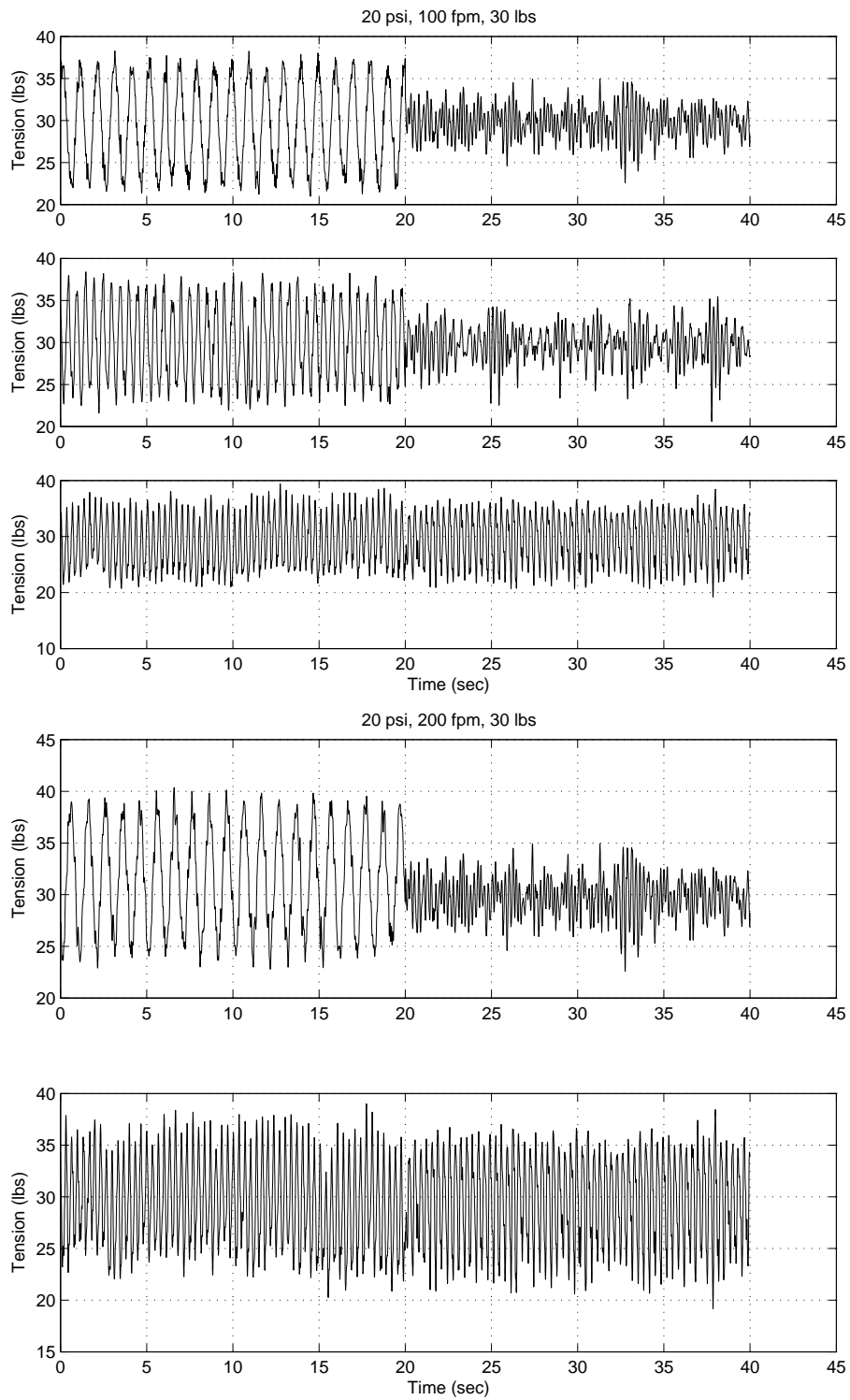


Figure A.7: Plots with disturbance attenuation at 100 and 200 fpm at 20psi

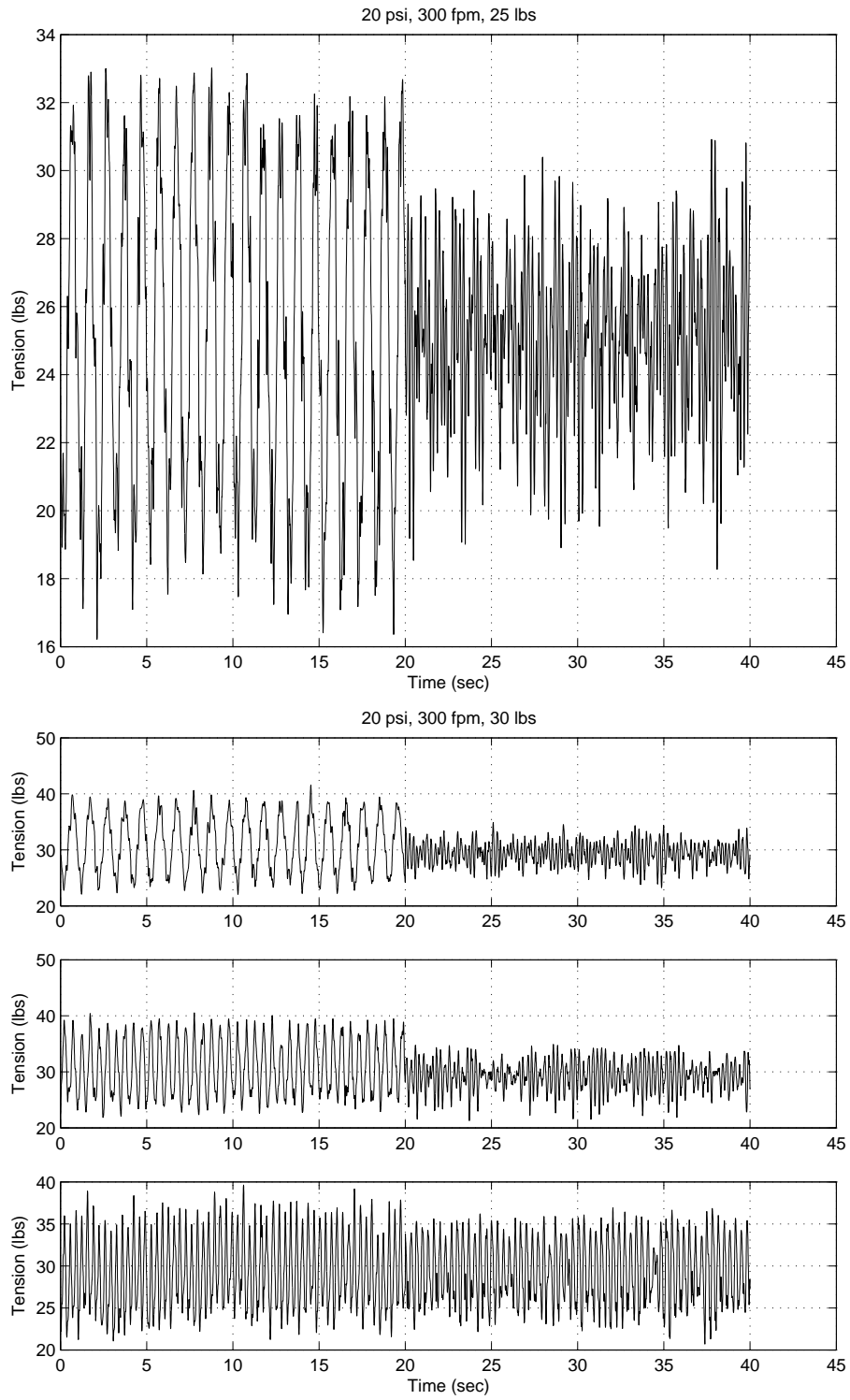


Figure A.8: Plots with disturbance attenuation at 300 fpm at 20psi

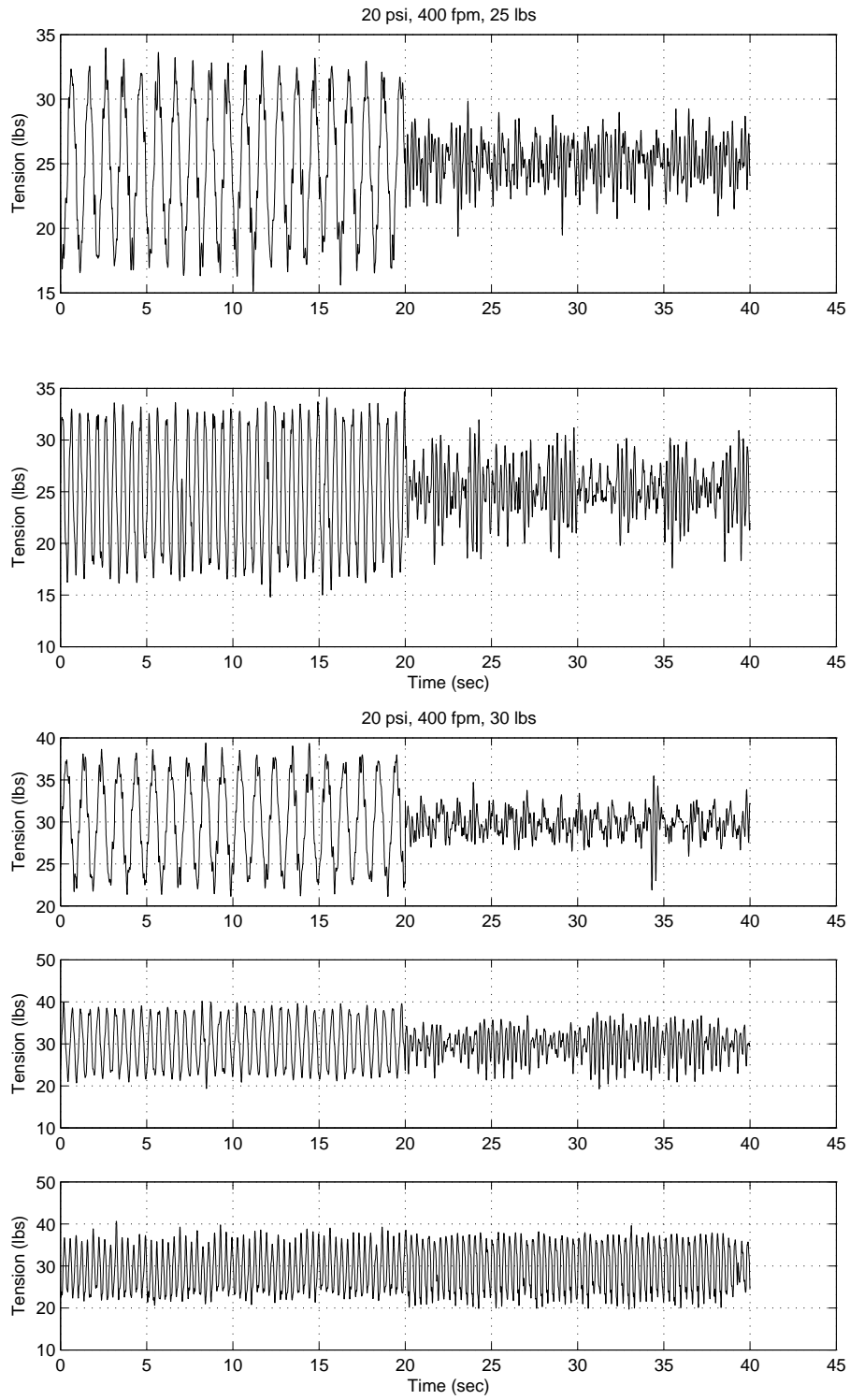


Figure A.9: Plots with disturbance attenuation at 400 fpm at 20psi

## APPENDIX B

### Experiments on White paper web

The following results are for the white “Tyvec” paper web.

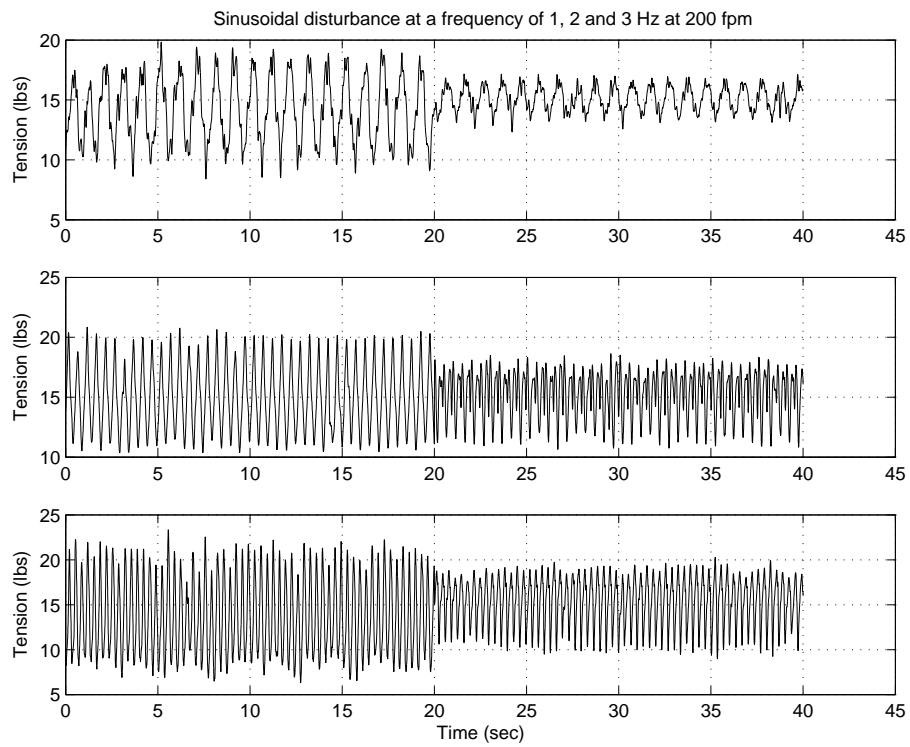


Figure B.1: Plot with disturbance attenuation at 200 fpm at 12psi

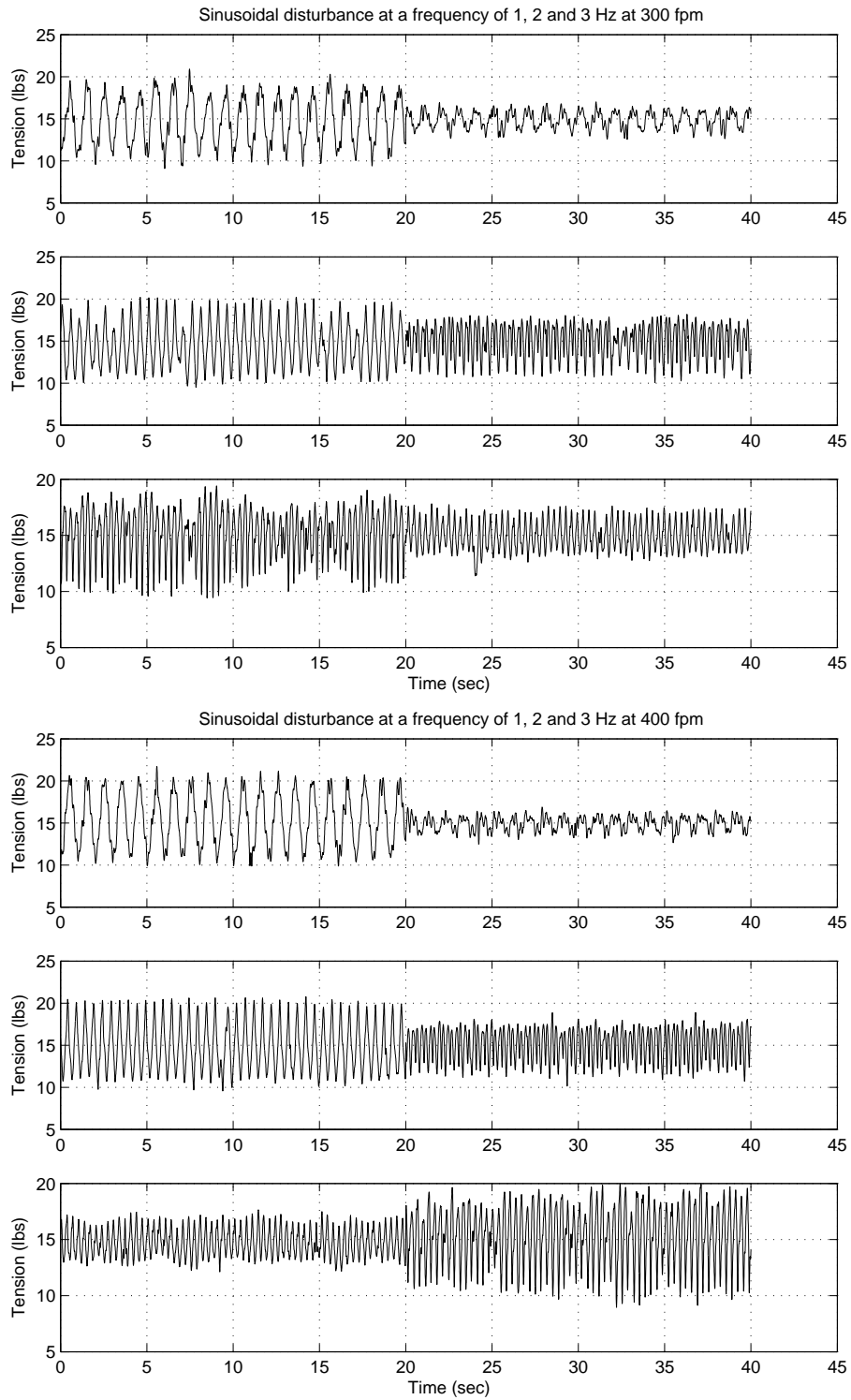


Figure B.2: Plots with disturbance attenuation at 300 and 400 fpm at 12psi

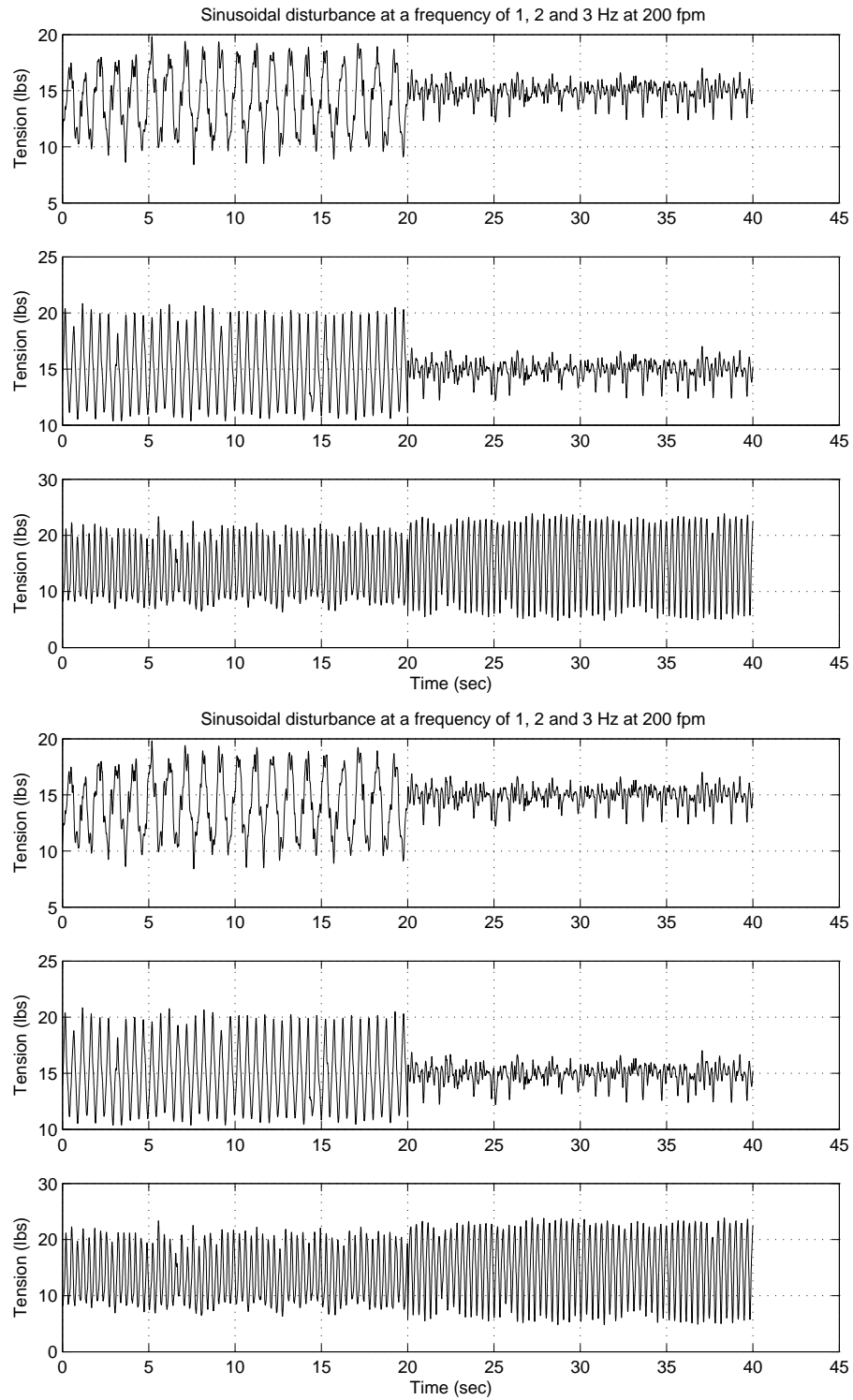


Figure B.3: Plots with disturbance attenuation at 100 and 200 fpm at 14psi

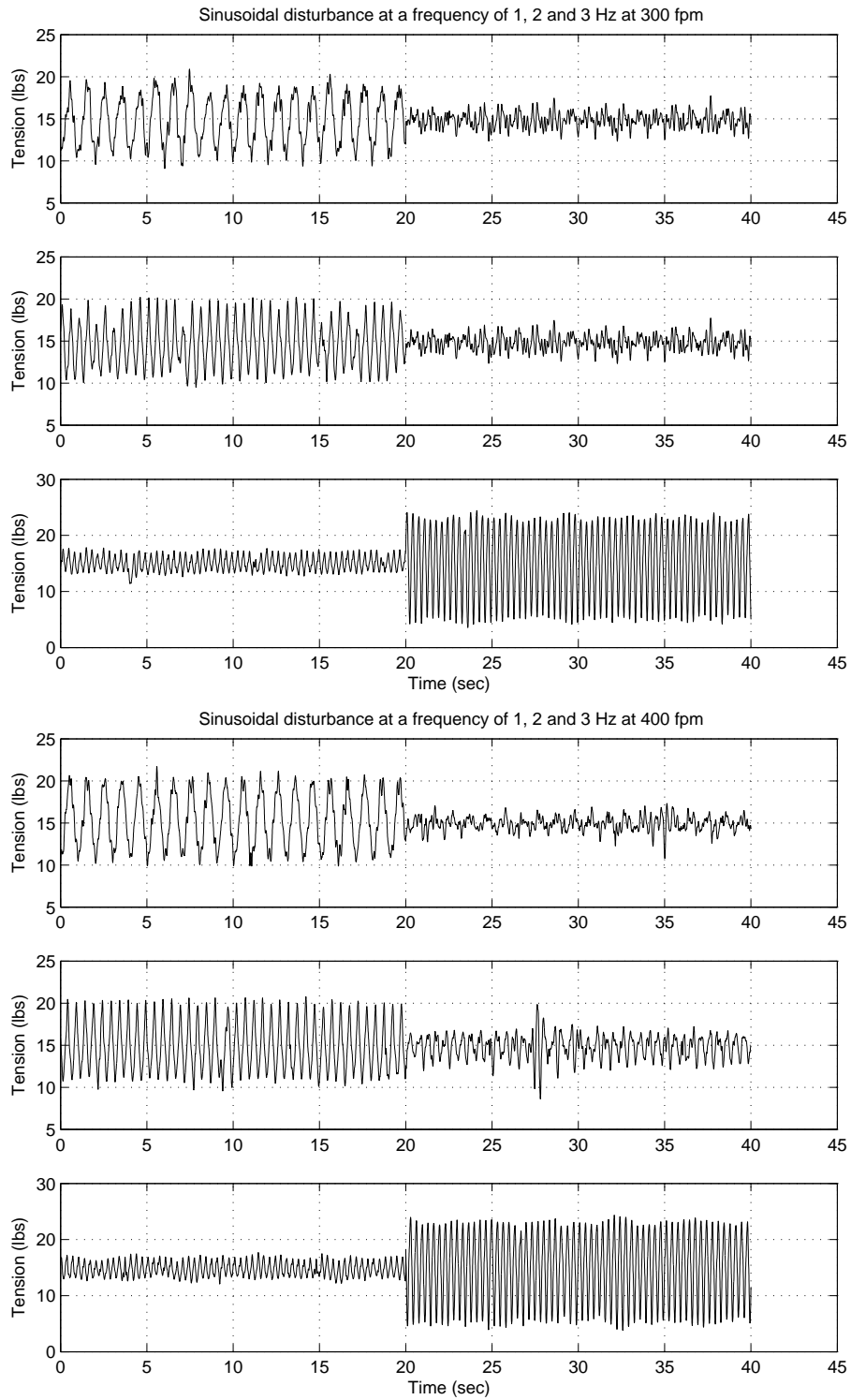


Figure B.4: Plots with disturbance attenuation at 300 and 400 fpm at 14psi



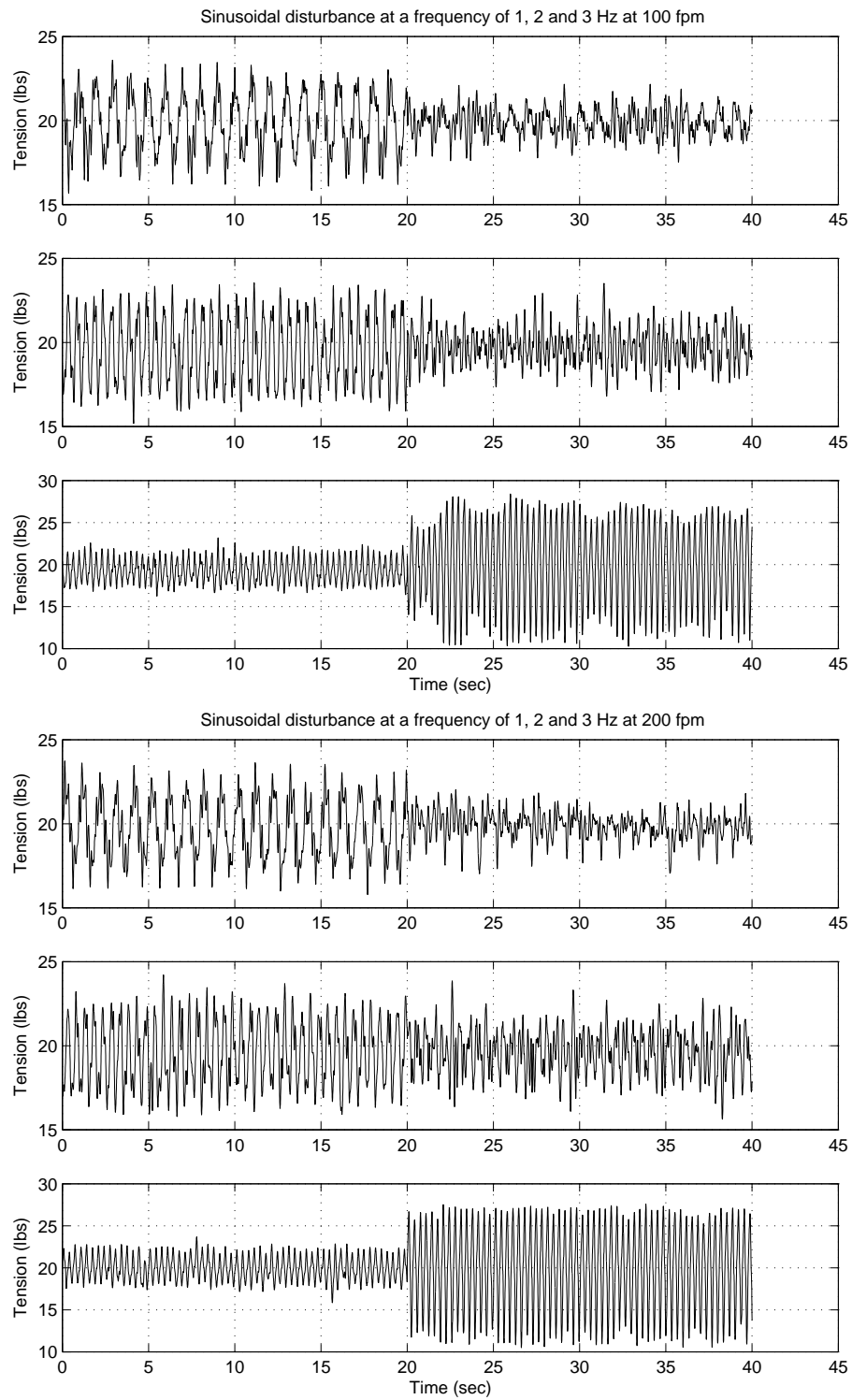


Figure B.5: Plots with disturbance attenuation at 100 and 200 fpm at 16psi

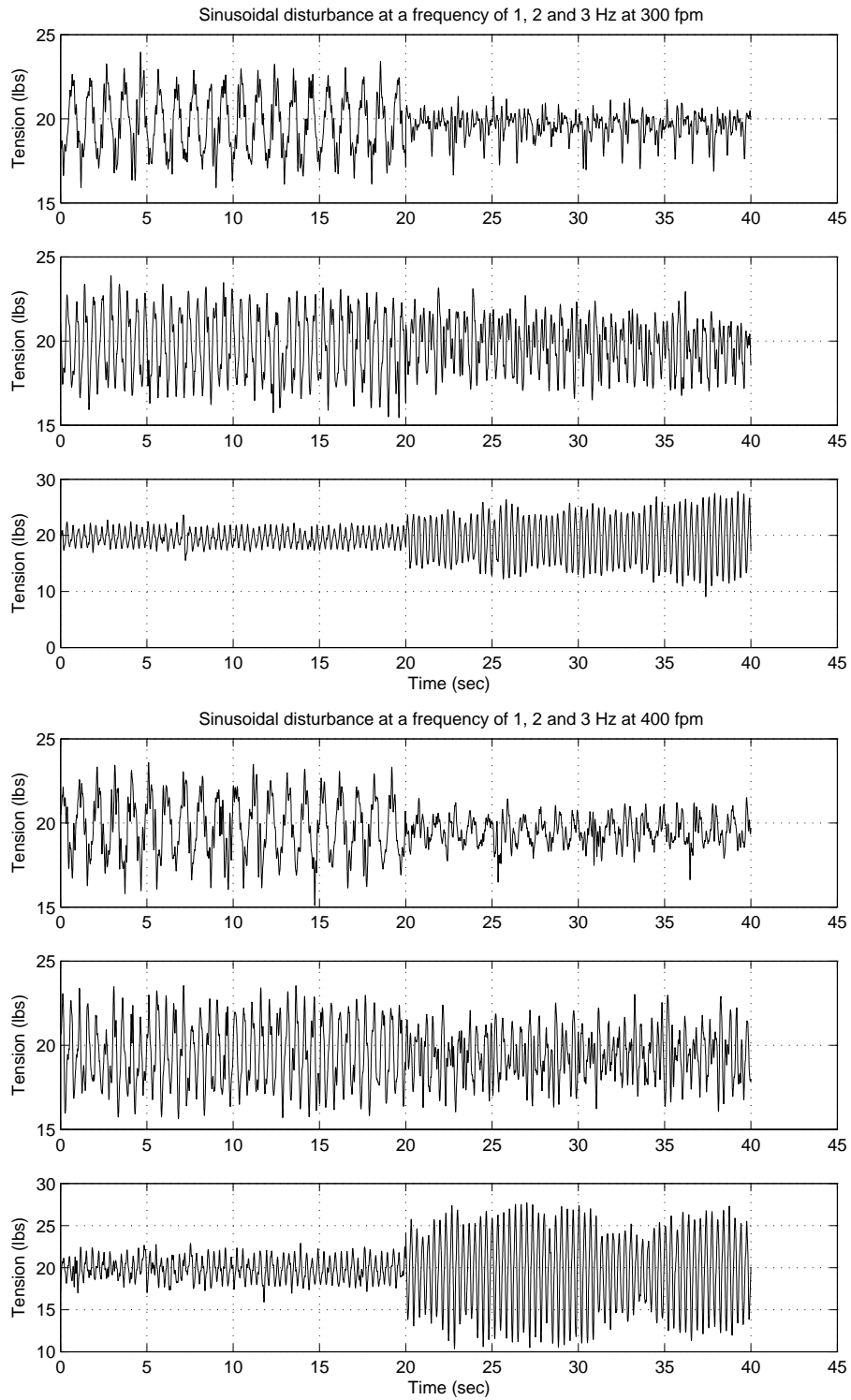


Figure B.6: Plots with disturbance attenuation at 300 and 400 fpm at 16psi

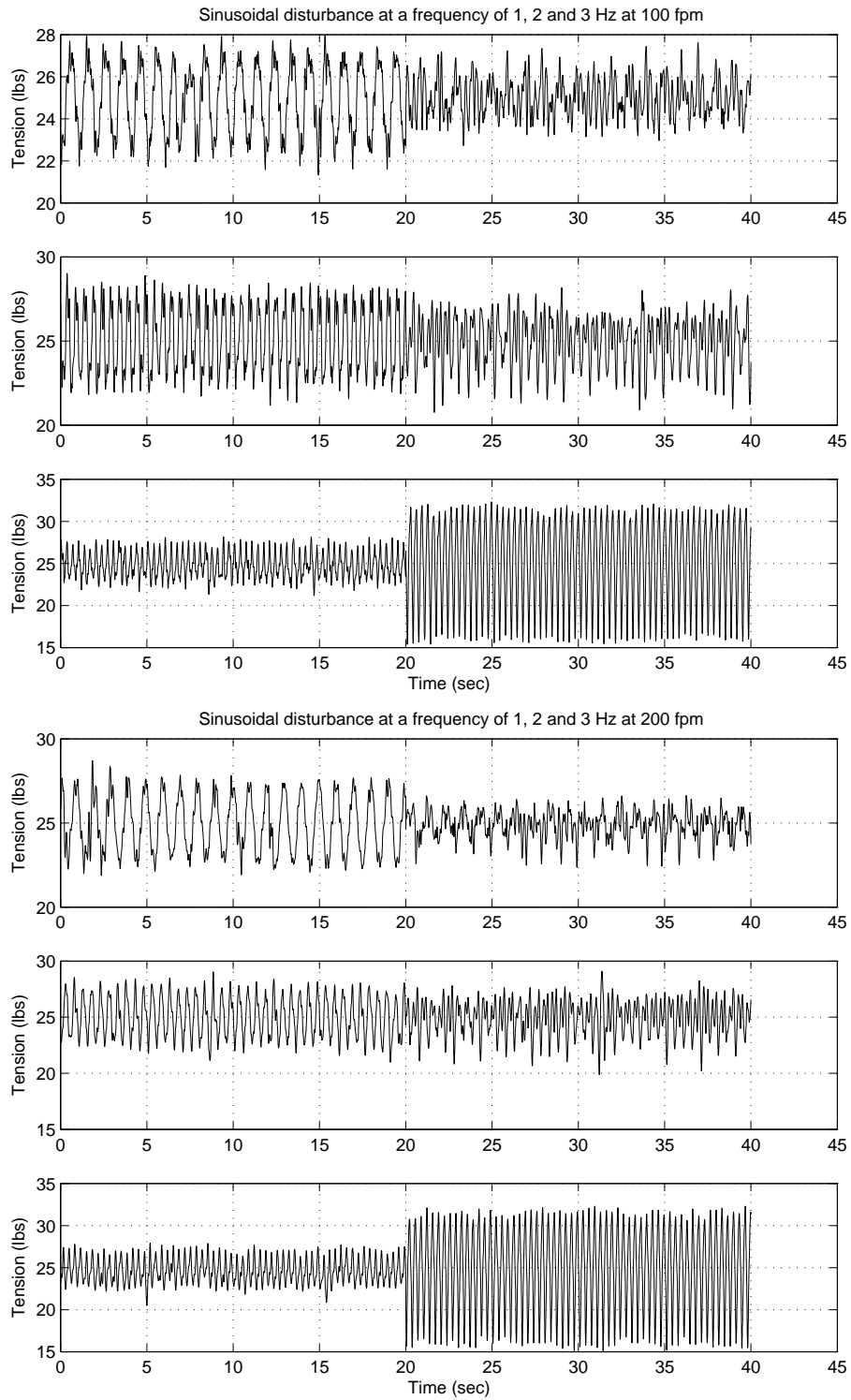


Figure B.7: Plots with disturbance attenuation at 300 and 400 fpm at 18psi

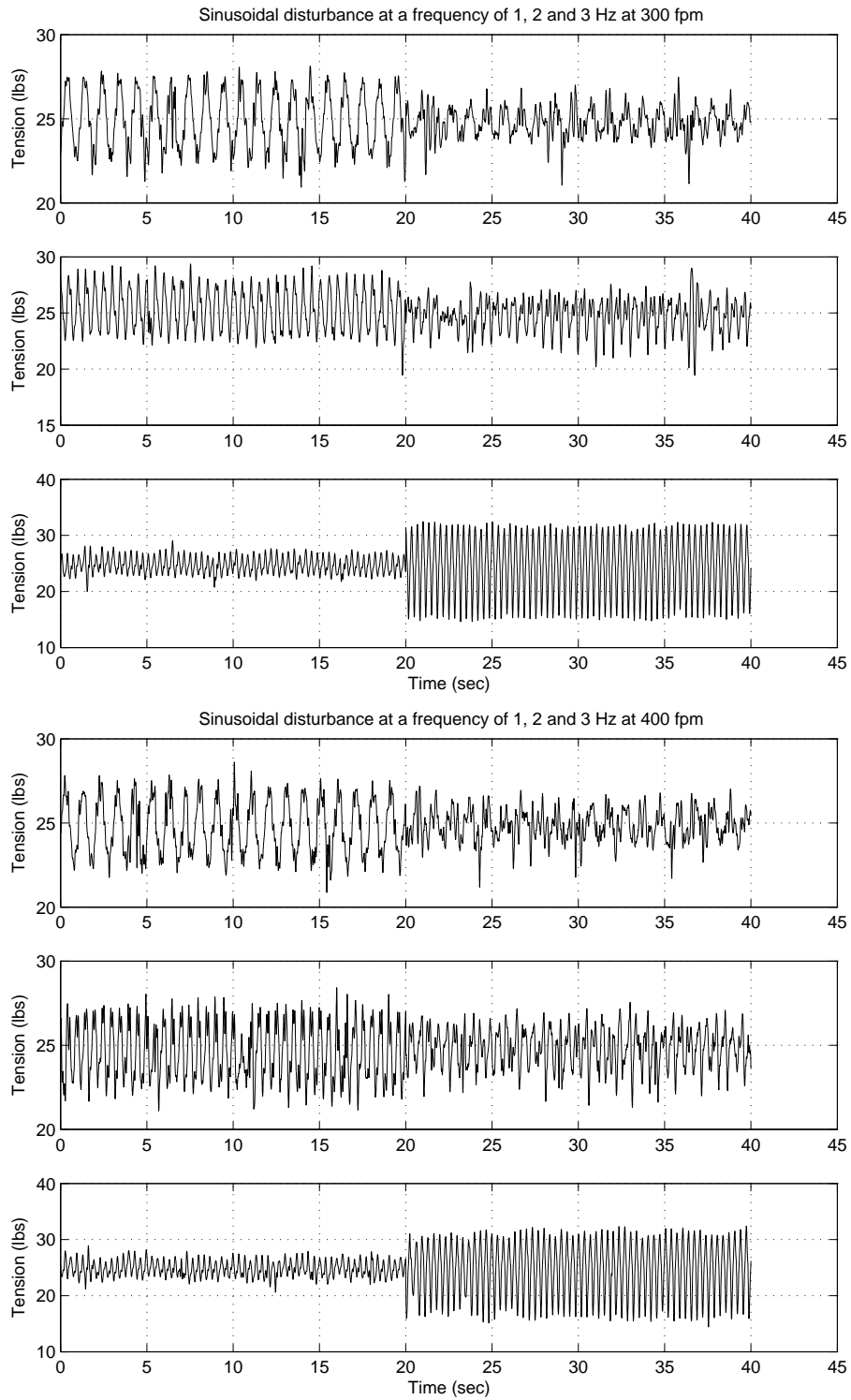


Figure B.8: Plots with disturbance attenuation at 300 and 400 fpm at 18psi

## APPENDIX C

### Calibration of sensors

This appendix contains the calibration of load cells and a tachometer followed by important functions like Filters and Voltage delimiters that protect the dSPACE board.

#### C.1 Downstream Load cell calibration

The downstream load cell is supported by an amplifier that gives it power and amplifies its signals before sending them to the data acquisition board.

The plot obtained after the calibration of the dancer downstream load cell is shown in the figure.

The equation for the plot is

$$V = \frac{(0.2198)2L}{0.8} - 0.8283$$

where  $V$  is the voltage and  $L$  is the tension/load in the web.

#### C.2 Dancer Load cell calibration

The Dancer load cell is also supported by an amplifier. It derives power from the amplifier and sends signals back to it. The amplifier directly plugs into the 115V AC power supply. The amplifier is a MAGPOWR product and its amplifier is very robust.

The plot obtained after the calibration of the dancer load cell is shown in the figure.

The equation for the plot is

$$V = (0.1877)2L - 0.0548$$

where  $V$  is the voltage and  $L$  is the tension/load in the web.

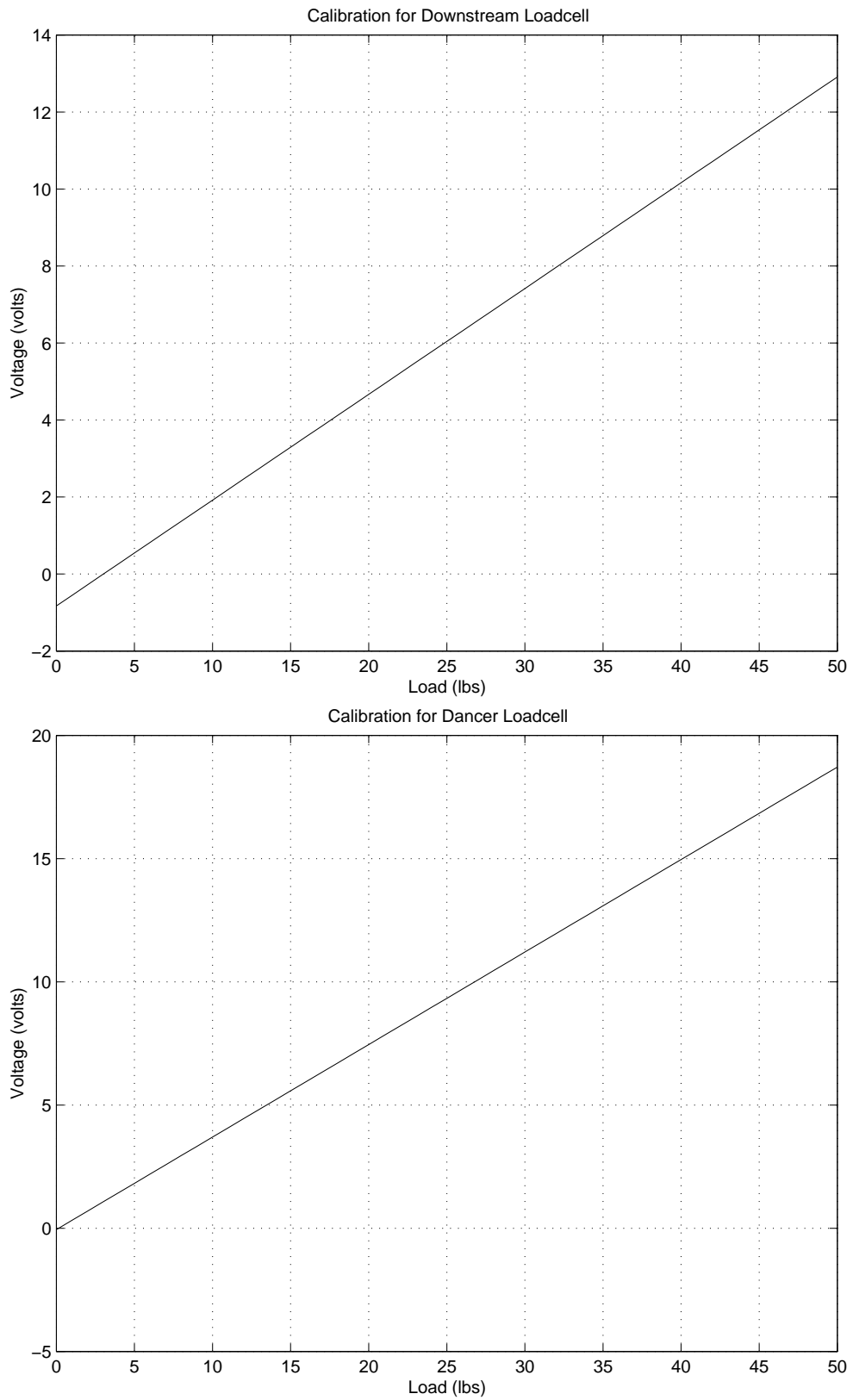


Figure C.1: Calibration plots for the Downstream and Dancer load cells respectively

### C.3 Disturbance Load cell

The disturbance load cell has an in built amplifier that directly plugs into a 12V DC supply. It directly gives out the signals to the data acquisition board. There is no external amplification required.

The plot shown below is obtained after the calibration of the disturbance load cell is shown in the figure.

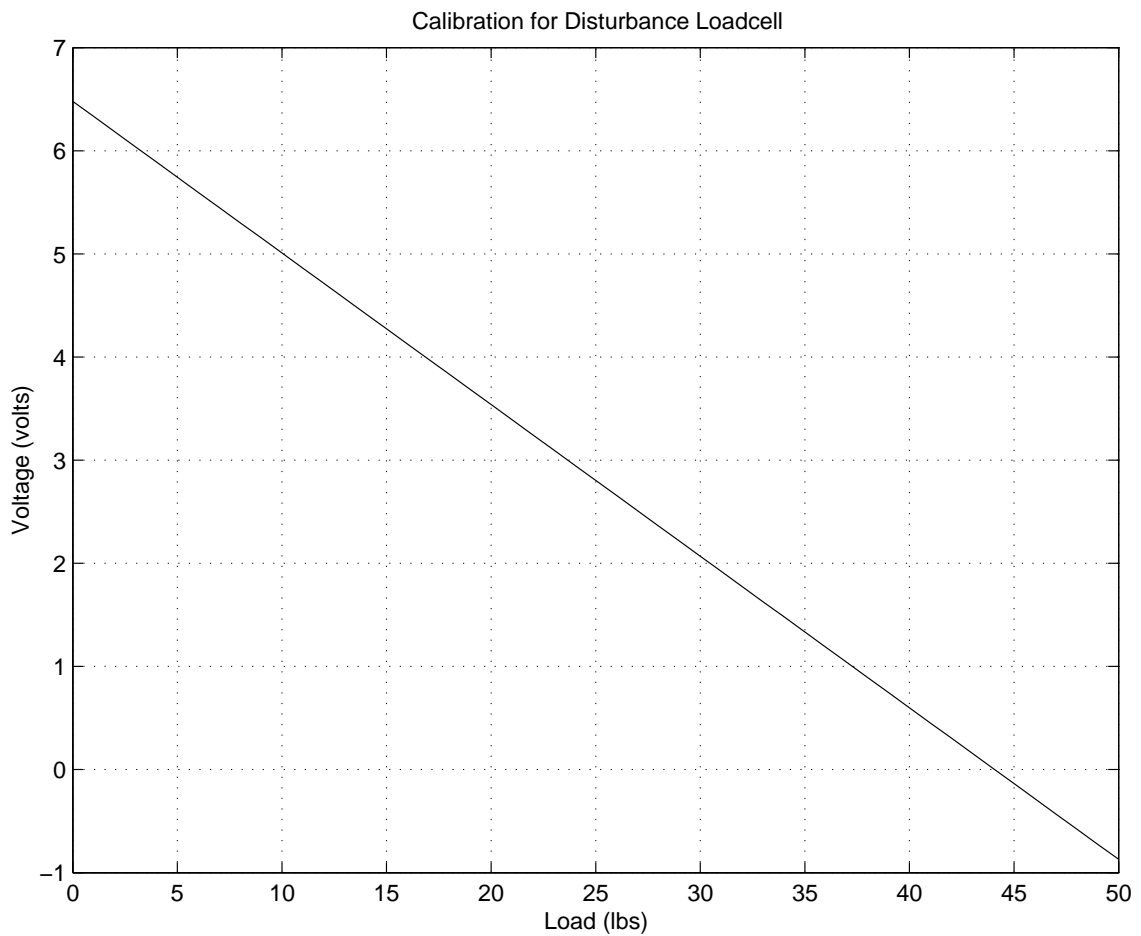


Figure C.2: Calibration plot of Disturbance load cell

The equation for the above plot is

$$V = (-0.0735)L + 6.4788$$

where  $V$  is the voltage and  $L$  is the tension/load in the web.

## C.4 Tacho-generator

The tacho-generator is attached to the master-speed driven roller using a roller fixed on its shaft. It absorbs power from the roller itself and the output voltage is proportional to the speed of the roller.

The plot obtained after the calibration of the dancer load cell is shown in the figure.

The equation for the above plot is

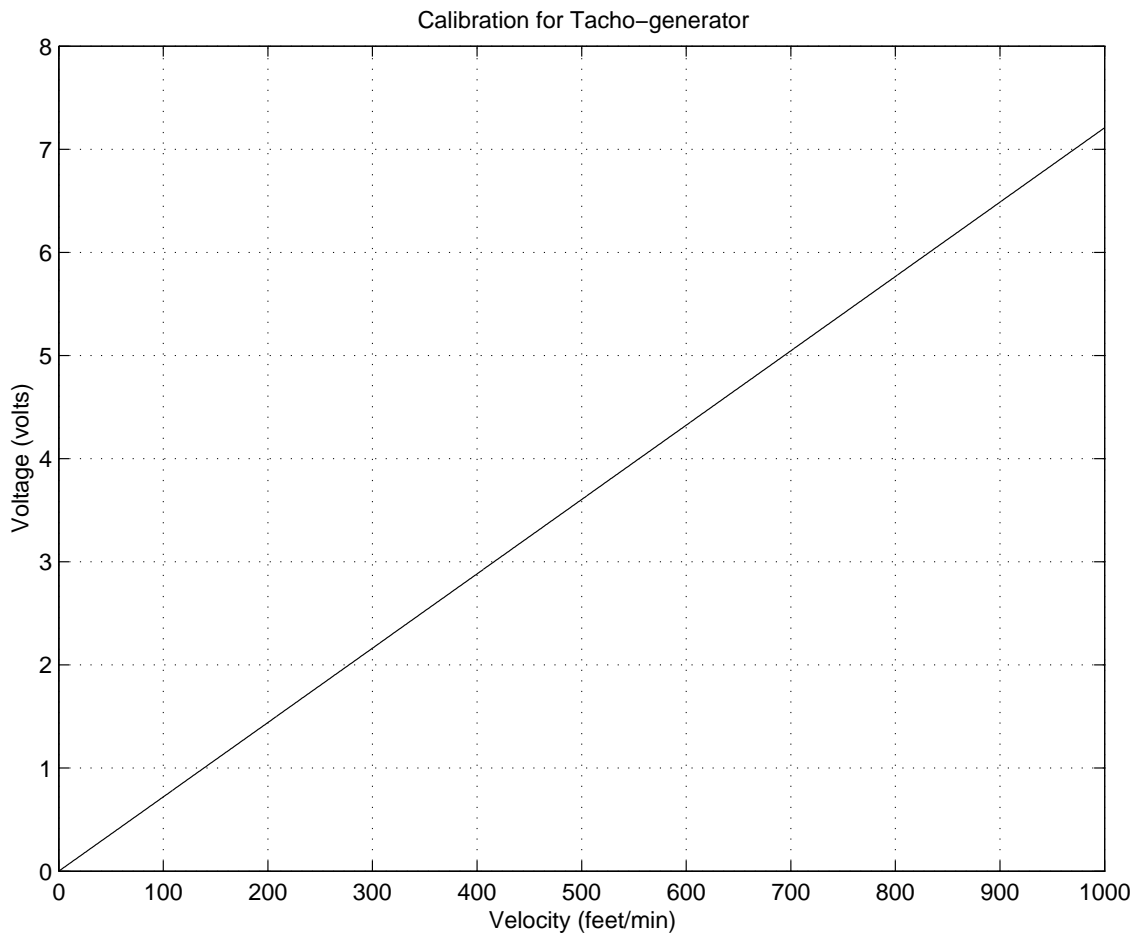


Figure C.3: Calibration plot of tacho-generator

$$V = (-0.0735)v + 6.4788$$

where  $V$  is the voltage and  $v$  is the velocity of the web.



## C.5 Low pass filter

A low pass filter has to be used to filter out the high frequency noises from the feedback signals. These signals may be from load cells, LDT or the tacho-generator.

Instead of using an RLC circuit, a similar digital filter can be designed and programmed depending on the frequency of noise to be attenuated. In this case a simple first order filter is used, that can be represented in the following continuous or discrete form.

$$\frac{Y(s)}{X(s)} = \frac{a}{s+a} \quad (\text{C.1})$$

$$\frac{Y(z)}{X(z)} = \frac{(1 - e^{-aT})z^{-1}}{1 - e^{-aT}z^{-1}} \quad (\text{C.2})$$

Simplifying back into time domain we get,

$$Y(z) = Y(z)e^{-aT}z^{-1} + X(z)(1 - e^{-aT})z^{-1} \quad (\text{C.3})$$

$$y(k) = y(k-1)e^{-aT} + x(k-1)(1 - e^{-aT}) \quad (\text{C.4})$$

The generic C program function for the filter is as shown.

```
Float64 filter_dist(Float64 x) //Dist(urbance) LC filter
{
    dist_tension_fil=
    (1-exp(-filter_coeff_dist*DT))*dist_tension_old
    +(exp(-filter_coeff_dist*DT))*dist_tension_fil_old;
    dist_tension_old=x;
    dist_tension_fil_old=dist_tension_fil;
    return dist_tension_fil;
}
```

## C.6 Voltage delimiter

The dSPACE board is designed to only read and send voltages between  $-10\text{volts}$  and  $10\text{volts}$ . So care has to be taken while sending actuator signals from the program to the board. Hence an output filter is designed to limit the voltages between  $-9.75\text{volts}$  and  $9.75\text{volts}$ .

The C program function for the delimiter function is as shown.

```
Float64 limit_output(Float64 x)
{
Float64 y;
if (x<=-9.75)
y=-9.75;
if(x>=9.75)
    y=9.75;
if((-9.5<x) && (x<9.5))
    y=x;
return y;
}
```

## C.7 Thermal Diffusivity

The thermal diffusivity of air used in calculation of the coefficients of the passive dancer gas spring transfer function, is found from the plot of Thermal diffusivity vs. temperature.

The points in this plot are values obtained from experiments. The equation for the best fit trendline is given as

$$y = 9.1018 \times 10^{-11} T^2 + 8.8197 \times 10^{-8} T - 1.0654 \times 10^{-5} \quad (\text{C.5})$$

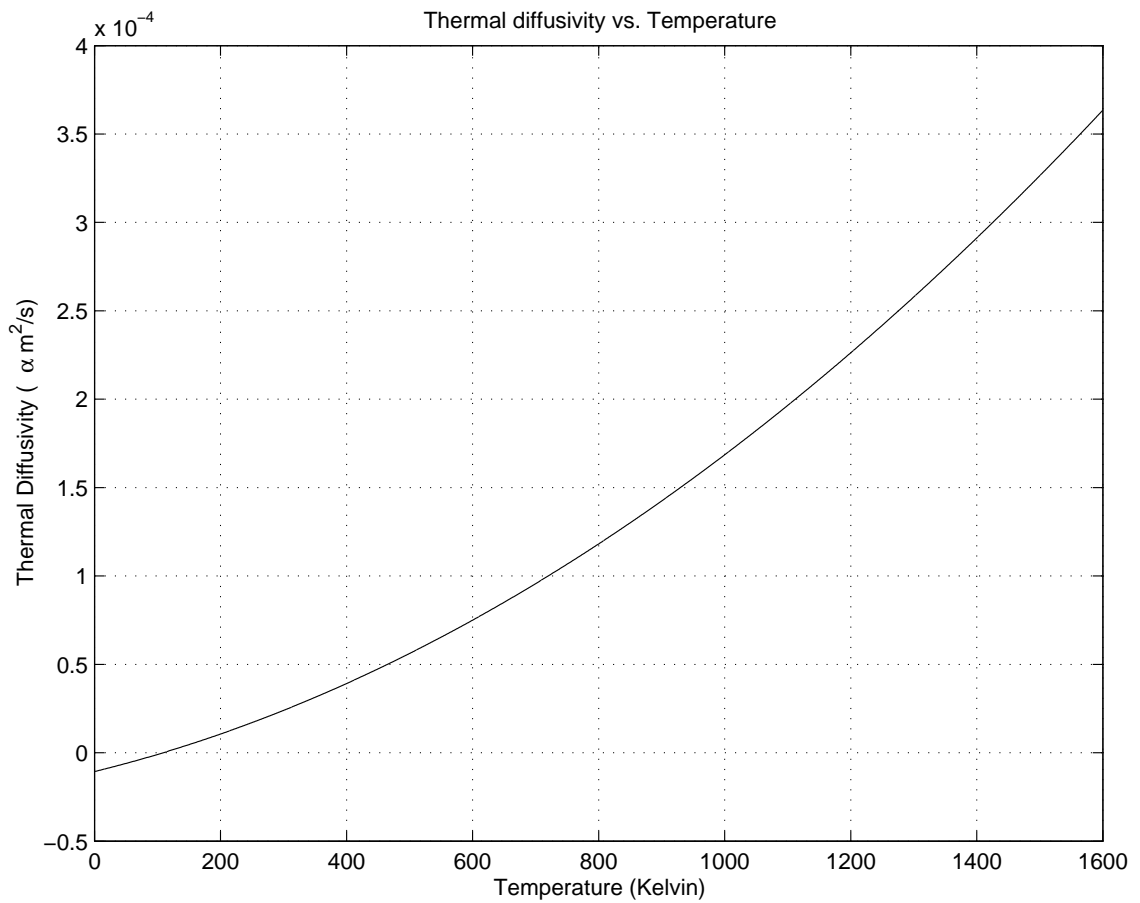


Figure C.4: Plot showing Thermal Diffusivity of Air vs. Temperature

## VITA

Seshadri Kuppuswamy

Candidate for the Degree of

Master of Science

Thesis: COMPARISON OF ACTIVE AND PASSIVE DANCERS FOR PERIODIC TENSION DISTURBANCE ATTENUATION IN WEB PROCESSING LINES

Major Field: Mechanical Engineering

Biographical:

Personal Data: Born in Mumbai, India, on December 12, 1974, the son of Kuppuswamy K.V. and Vasanthi Kuppuswamy.

Education: Received the B.E. degree from University of Mumbai, Mumbai, India, in 1997, in Mechanical Engineering; Completed the requirements for the Master of Science degree with a major in Mechanical Engineering at Oklahoma State University in December, 2004.

Experience: Research Assistant at Oklahoma State University from January 2002 to August 2004; Teaching Assistant at Oklahoma State University from January 2002 to December 2003; Tool-Room Engineer at M/s Earl Bihari Pvt. Ltd., Mumbai, India from Sept 1999 to March 2001; Intern at Bhabha Atomic Research Center, Mumbai, India from June 1996 to May 1997.

Professional Memberships: American Society of Mechanical Engineers.

Name: Seshadri Kuppuswamy

Date of Degree: December, 2004

Institution: Oklahoma State University

Location: Stillwater, Oklahoma

Title of Study: COMPARISON OF ACTIVE AND PASSIVE DANCERS FOR PERIODIC TENSION DISTURBANCE ATTENUATION IN WEB PROCESSING LINES

Pages in Study: 81

Candidate for the Degree of Master of Science

Major Field: Mechanical Engineering

Scope and Method of Study: This thesis compares the performance of passive and active dancers in a web process line in the presence of periodic tension disturbances. A sinusoidal disturbance, injected into the web line using an eccentric roller, is attenuated using the passive and active dancers. The piston-cylinder for the passive dancer is modeled as a gas spring with air as the compressible fluid and a model is suggested. The active dancer setup is fitted with a hydraulic actuator and the experiments are conducted for attenuation using a PID and an IMC controller.

Findings and Conclusions: It is seen that the passive dancer mechanism is effective in attenuating web-tension at lower frequencies of disturbance. Its response to tension variations and its attenuation capabilities are limited due to the properties of its passive elements and its damped natural frequency. The properties of a passive dancer can be slightly varied using a gas spring and varying the pressure of the gas. This limitation is overcome by the active dancer with an actuator. The electro-hydraulic actuator, used in the active dancer has a high bandwidth compared to the electro-mechanical actuator. The IMC controller is found to be satisfactory in attenuating the sinusoidal disturbance up to a disturbance frequency of  $28 \text{ rad/sec}$  and easier to design than the PID controller.

ADVISOR'S APPROVAL: \_\_\_\_\_